Progress in Materials Science 144 (2024) 101287

Contents lists available at ScienceDirect

Progress in Materials Science

journal homepage: www.elsevier.com/locate/pmatsci

Emerging 2D materials beyond mxenes and TMDs: Transition metal carbo-chalcogenides

Kassa Belay Ibrahim [a,*], Tofik Ahmed Shifa [a], Sandro Zorzi [a], Marshet Getaye Sendeku [b], Elisa Moretti [a,*], Alberto Vomiero [c,*]

[a] Department of Molecular Sciences and Nanosystems, Ca' Foscari University of Venice, Via Torino 155, 30172 Venezia Mestre, Italy
[b] Ocean Hydrogen Energy R&D Center, Research Institute of Tsinghua University in Shenzhen, Shenzhen 518057, PR China
[c] Division of Materials Science, Department of Engineering Sciences and Mathematics, Luleå University of Technology, SE-97187 Luleå, Sweden

ARTICLE INFO

Keywords:
TMD
MXenes
Transition metal carbo-chalcogenides
Carbo-sulfides
New family of 2D material

ABSTRACT

The discovery of graphene sparked significant interest in 2D materials, which present an ultra-thin layered structure with high anisotropy and adjustable energy-band structure. Interestingly, it opens the door for the development of the 2D materials family, which includes different classes of 2D materials. Among them, transition metal dichalcogenides (TMDs) and transition metal carbide MXenes (TMCs) have emerged. TMDs have unique layered structures, low cost, and are composed of earth abundant elements, but their poor electronic conductivity, poor cyclic stability, their structural and morphological changes during electrochemical measurements hinder their practical use. Recently, TMC MXenes have garnered attention in the 2D material world, but the issue of restacking and aggregation limits their direct use in large-scale energy conversion and storage. To address these challenges, hetero structures based on conductive TMCs MXenes and electrochemically active TMDs have emerged as a promising solution. However, understanding the solid/solid interface in heterostructured materials remains a challenge. To tackle this, 2D single component crystals with high capacity, low diffusion barrier, and good electronic conductivity are highly sought. The emergence of transition metal carbo-chalcogenides (TMCCs) has provided a potential solution, as these 2D nanosheets consist of TM_2X_2C, where TM represents transition metal, X is either S or Se, and C atom. This new class of 2D materials serves as a remedy by avoiding the challenges related to solid/solid interfaces often encountered in heterostructures. This review focuses on the latest developments in TMCCs, including their synthetic strategies, surface/interface engineering, and potential application in batteries, water splitting, and other electro-catalytic processes. The challenges and future perspectives of the design of TMCCs for electrochemical energy conversion and storage are also discussed.

1. Background

The pressing issues of energy and environment are among the top challenges facing our society. Environmental pollution and the energy crisis have highlighted the need for catalysts that can efficiently degrade pollutants, reduce CO_2 emissions, and generate carbon-free energy. One promising approach to generating hydrogen from renewable sources is through water electrolysis, which

* Corresponding authors.
E-mail addresses: kassabelay.ibrahim@unive.it (K. Belay Ibrahim), elisa.moretti@unive.it (E. Moretti), alberto.vomiero@ltu.se (A. Vomiero).

https://doi.org/10.1016/j.pmatsci.2024.101287
Received 31 October 2023; Received in revised form 5 March 2024; Accepted 19 March 2024
Available online 20 March 2024

involves the oxygen evolution reaction (OER) and Hydrogen evolution reaction (HER) as the core electrochemical reactions. Similarly, fuel cells can convert hydrogen energy to electricity with zero emissions, making them highly efficient and clean. In both cases, catalysis plays a crucial role.[1] The development of "Green Hydrogen" from photo-/electro-catalytic water splitting is seen as a key solution for meeting the global goal of net-zero carbon emissions by 2050. It represents a sustainable energy source that can help reduce our dependence on fossil fuels and minimize CO_2 emissions. As such, catalysis is essential in this effort to achieve a cleaner, more sustainable future. [2–5] In recent years, research on 2D materials, [6] has expanded beyond graphene to include other van der Waals (vdW) materials such as TMDs, TMC MXenes, and heterostructures of TMCs and TMDs. [7] This review provides an overview on the advancements in 2D materials, from TMDs and TMC MXenes to the new family of TMCCs in the field of energy conversion and storage. TMCCs present a promising way to bridge the gap between TMC MXenes and TMDs. Although various families of layered ternary materials such as TMDs and TMC MXenes have been extensively studied, the search for inorganic porous materials that substitute precious metals has not been adequately addressed until recent years.

2. Transition metal dichalcogenides (TMDs)

TMDs are a class of materials composed of transition metals and chalcogens. [8] TMDs are composed of transition metals from group IIIB to group VIIIB of subgroup elements in the element periodic table (Ti, Pt, V, Zr, Nb, Mo, Hf, Ta, W etc) and S or Se of the group VIA in a 1:2 ratios. [9,10] TMDs have attracted a significant attention due to their unique electronic, optical, and catalytic properties, which make them promising candidates for a wide range of applications, such as solar cells, thermoelectric devices, superconductors, and catalysts. However, poor conductivity of these 2D TMDs significantly inhibits their electrochemical performances. Some examples of TMDs include SnS_2, MoS_2, WS_2, and FeSe. MoS_2, for example, is a two-dimensional material with a layered structure that has shown promising potential for use in electronic devices, particularly as a field-effect transistor. WS_2 has a similar layered structure to MoS_2 and has been found to exhibit high mechanical strength and high thermal stability.

Transition metal chalcogenides (represented by MX_2, M = Mo, Zr, Ge, Sn, V, Cr, Nb, W, Re, Ti and X = S, Se, Te) such as MoS_2, SnSe, $MoTe_2$, FeS, SnS, GeSe, and GeS, WSe_2, TiS_2, ZrS_2 etc). In layered TMDs, the M layer is sandwiched between two chalcogenides (X) layers resulting in an MX_2 stoichiometry. The interlayer bonds between two MX_2 slabs are vdW bonds. As shown in Fig. 1a, TMDs can exist in the form of trigonal prismatic or octahedral structure (or 2H and 1 T phase) depending on the transition metal coordination by the chalcogenide and the stacking sequence of multilayers. The most found TMD polymorphs are 2H, 1 T, and 3R standing for hexagonal (or trigonal prismatic), tetragonal (or octahedral) and rhombohedral symmetry. The thermodynamic stability of the different TMD phases can vary depending on the transition metals. [11] The most widely studied group VIB bulk TMDs (e.g. MoS_2, WSe_2, $MoTe_2$) exhibit 2H or 3R phase [12–16], the group VB TMDs (e.g. TaS_2,$TaSe_2$) exhibit 2H or 1T phase [17–21], and all the group IVB TMDs (e.g. TiS_2, ZrS_2) are 1T phase [22–26]. It has been found that phase changes can be induced by intercalation [27–32]. These structural phases featured with different symmetries and stacking orders, relating to the d-electron count that affect band structures, primarily play important roles in affecting the electronic properties. Furthermore, the crystal structure of single-layer TMDs (MX_2) comprises a transition metal layer sandwiched between two atomic layers of chalcogen. This class of low-dimensional materials and their hetero-structures are an ideal platform for multiple applications in electronics, and optoelectronics owing to their numerous unique physical and chemical properties such as high electron mobility, thermal conductivity, unconventional superconductivity, piezoelectricity, and giant magnetoresistance [33–36]. However, the physical and chemical properties of as-grown 2D TMDs often do

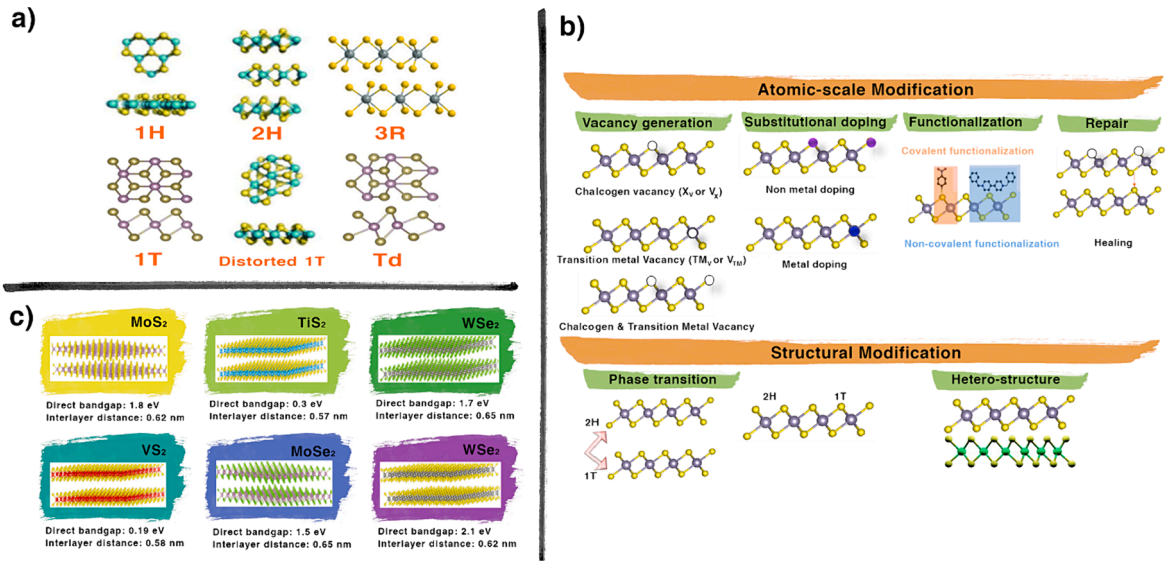

Fig. 1. (a) Structure polytypes of layered TMDs (b) Summary of atomic-scale and structural modifications of 2D TMDs and vdW hetero-structure (c) bandgap and interlayer distance of various types of TMDs.

not meet the specific requirements for advanced applications. Thanks to anisotropic layered structures, the electronic structures of 2D TMDs can be modified by multiple factors [37] such as thickness thinning down, vacancy generation [38,39], foreigner species interaction [40–42], surface functionalization [43–45], external strain [46,47], substitutional doping [48,49], and stacking or assembling hetero structures [50,51] (Fig. 1b). The activated basal planes and edge sites of 2D TMDs are reported as highly active toward hydrogen and oxygen catalysis [52,53]. On the other hand, with the rapid developments of large-scale preparation technology, considering the preparation methods such as chemical exfoliation, CVD, printing techniques, and so on, 2D TMD materials show the great potential for different applications. Therefore, designing hetero-structures of materials composed of different 2D TMDs stacked along the out-of-plane direction (vertical heterostructure) or in-plane direction (lateral structure) is a common approach to modify the electronic band structures of the materials [54–56]. Depending on the d-electron counts, TM elements can result in a wide variety of electronic properties including insulators, semiconductors (MoX_2 and WX_2) having partially filled group VIB [57,58], semimetals, metals (NbX_2 and TaX_2 that has fully filled group VB) [59,60], and superconductors. Semiconducting TMDs possess bandgaps in the near-infrared to the visible region, that makes them promising in optoelectronics and photonics applications [61–63]. However, compared to bulk TMDs, the electronic properties of 2D TMDs are considerably tuned as a result of quantum confined effect in the out-of-plane direction [64,65]. The choice of electrode materials plays a critical role in the electro/photocatalyst for water splitting and the anode material for Li-ion batteries. It is essential for ion transport and the overall electrochemical performance. In this context, compounds based on TMDs like Fe-MoS_2 [66], MoS_2/CoS_2 [67], NiSe [68], $MoWS_2/Ni_3S_2$ [69], Co/MoS_2 [70], $CoTe_2$@Ni [71], and $NiTe_2$/Ni $(OH)_2$ [72] are viewed as promising materials for achieving superior performance in OER and Li-ion batteries like 2D MoS_2 nanosheets [73], 2D SnS_2 nanoplates [74], Mo doped SnS_2 on carbon [75], SnS_2/MoS_2 on carbon [76], MoO_3/SnS_2 core shell nanowire [77], WS_2 nanosheets [78] and VS_2/graphene nanocomposites [79]. These materials exhibit high conductivity, high surface area, remarkable flexibility, a robust polar surface, and a propensity to accommodate various cations.

Owing to the weak vdW force, the ions can diffuse rapidly through the interlayer gap of MX_2 layer. The large interlayer distance between the MX_2 layer makes it possible to accommodate multivalent ions such as Zn^{2+}, Mg^{2+}, Al^{3+}, and Ca^{2+}.The interlayer distance and bandgaps of various TMDs is reviewed in Fig. 1c. TMDs suffer from intrinsically poor electrical conductivity, large volume changes upon cycling poor cycling stability, and, most importantly, a limited number of active sites located on the edges, which utterly restricts the catalytic performance [80–85]. In recent years, there has been growing interest in TMCs for their unique electronic and optical properties, as well as their potential for use in a variety of applications. However, further research is needed to fully understand the properties of these materials and to develop new and improved applications for TMCs.

3. Transition metal carbide MXenes (TMC MXenes)

One of the latest, and relatively large, family of 2D materials is transition-metal carbides and nitrides, called MXenes. MXenes (pronounced as maxenes) [86–88] are demonstrated by the chemical formula $M_{n+1}X_nT_x$, where M represents Ti, V, Mo), X is C and/or N (n = 1, 2 or 3), and T_x is the surface-terminating functionality (e.g., −O, −OH, and/or − F). $Ti_3C_2T_x$ the first TMC MXenes family were discovered in 2011 and has greatly expanded and made an impact in the fields of energy [89]. Thanks to Gogotsi's group efforts TMC MXenes has become a promising area of research [90]. TMC MXenes are an interesting class of materials as electrocatalyst since

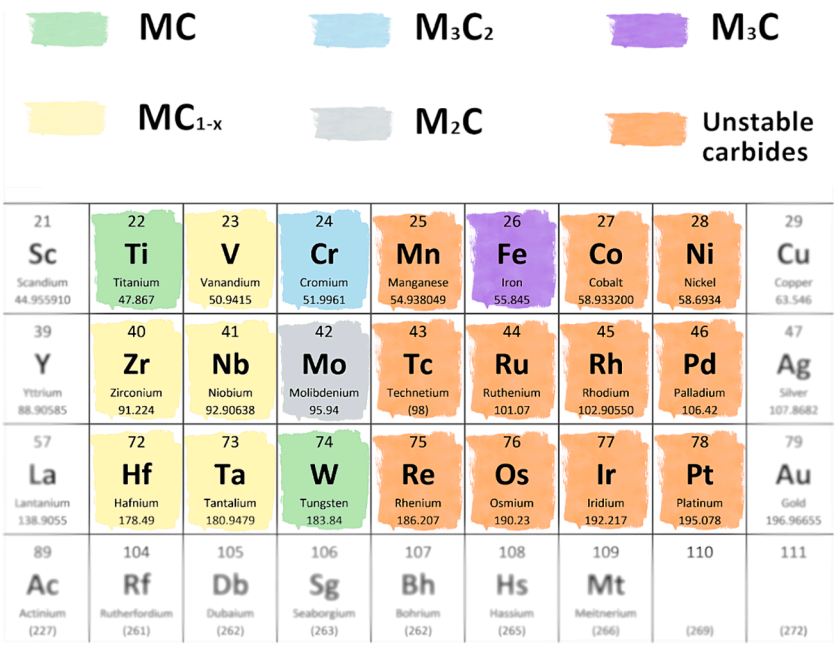

Fig. 2. Different groups of Transition metals and their thermodynamically stable carbide formations.

they are chemically stable in acidic media, resistant to poisoning, have excellent mechanical durability and possess high electronic conductivity. MXenes, which are single layered counterparts of non-layered TMC, were proposed to be the promising anode materials for metal ion batteries because of their good conductivity [91–93]. Due to this, MXenes are a rapidly expanding family of 2D TMCs, offering enormous structural and chemical diversity. Owing to the free electrons of the TMC skeleton and the surface groups, MXenes demonstrate good electronic conductivity and hydrophilicity, leading to their wide application range, including batteries, capacitors, catalysts, adsorption, and water purification. Although this compositional variability allows fine-tuning of the MXene properties, it also creates challenges during the analysis due to the presence of multiple light elements (such as H, C, N, O, and F) in proximity. Most transition metals, apart from Pt-group metals, form carbides. Moreover, as can be seen in Fig. 2, the carbides of elements neighboring the Pt group metals are not stable, with the exception of Fe carbide [94]. The carbides of Group 4–10 are thermodynamically more stable and possess catalytic properties greatly improved over those of parent transition metals [94–96]. As a result, the MXenes family is quite diverse with multiple forms: single metal structures ($Ti_3C_2T_x$, Ti_2CT_x, V_2CT_x, etc.), ordered double TM MXenes (i.e., $Mo_2Ti_2C_3T_x$, $Mo_2TiC_2T_x$, $Cr_2TiC_2T_x$, etc.), solid solution MXenes (i.e., $Ti_{2-y}V_yCT_x$, $Mo_{4-y}V_yC_3T_x$, $Ti_{2-y}Nb_yCT_x$), and ordered divacancy MXenes ($Mo_{1.33}CT_x$, $W_{1.33}CT_x$, etc) [93,97,98]. This variety results from the change in the M or X elements, the modification of the number of atomic layers (n), adjusting the surface chemistry (T_x) through post-treatment or during synthesis, and intercalation of different species into the structure [89]. Generally, MXenes have a unique combination of properties that make them desirable for energy storage applications due to, at least, the following reasons: (i) The surface terminations, more specifically -O, create transition metal oxide like surfaces, which are redox active. (ii) MXenes possess high electrical conductivity. This conductivity provides fast transport of electrons to the electrochemically active sites. (iii) MXene layered 2D nature and the ease of cation intercalation leads to fast ion transport [99–101]. A widely acknowledged precursor for Mxenes are a class of compounds known as MAX phase (such as Ti_3SiC_2, Ti_3AlC_2, V_2AlC, Ti_4AlN_3, etc.) that are categorized as layered ternary carbides and nitrides. These materials are predominantly explored and developed in the field of structural ceramics. By selectively extracting/etching the A layer from MAX phases, one can obtain a unique class of materials known as metal carbides (such as Ti_2C, V_2C, Fe_2C, Ti_3C_2,Nb_2C, Mo_2C, Cr_2C, Ta_2C, Ti_3C_2, Hf_3C_2 Cr_3C_2, Nb_4C_3, $Mo_{1.33}C$, Cr_2N, Ti_4N_3, Ti_3CN, $(V_{0.5},Cr_{0.5})_3C_2$, $(Ti_{0.5}\,Nb_{0.5})_2C$, Mo_2ScC_2, $Mo_2Ti_2C_3$, $(Nb_{0.8}Ti_{0.2})_4C_3$ and $(Nb_{0.8}Zr_{0.2})_4C_3$) [90,102,103], which possess a 2D structure. Based on this, different families of Mxene have been developed as water oxidation and anode material for Li ion battery.

4. Metamorphosis of MAX to MXenes

The MAX phases ($M_{n+1}AX_n$) and their derivatives, MXenes, are a class of materials that combine the important properties of metallic and covalent bonding, with a lamellar structure and weak bonds between M and A layers (Fig. 3a) [104]. They exhibit unique combinations of properties, including high electrical and thermal conductivity, low density, mechanical strength and significant effective anisotropic movement of electron (e^-) and hole (h^+) [105]. The first chemically ordered MAX phase alloy was discovered in 2014 [106,107], and currently, over 150 MAX phases and more than 30 MXenes with three types M_2XTx, M_3X_2Tx, and M_4X_3Tx (Fig. 3b) have been reported with different compositions. The MAX phases have a nanolayered hexagonal structure with P63/mmc symmetry, prototype Cr_2AlC, where the M layers are nearly closely packed, A is a group of elements, and X is carbon atoms filling the octahedral sites [108,109]. M_2A_2X has an extra A layer resulting in a change in the lattice constant c. In this framework, Mo_2Ga_2C is a new compound with two Ga layers instead of one in Mo_2GaC and other MAX phases. These phases exhibit superconductor properties, and transition metals such as Mn, Fe, Cu, Zn, Cd, Ir, and Au can become the A layer of MAX phases [110,111]. However, MXene with pure Mn as the M has not been synthesized from a MAX phase yet. A lutetium-containing MAX phase (Lu_2SnC) has been synthesized adding the possibility of having lanthanides as MAX phase components [112]. MXenes can be synthesized from MAX phases via

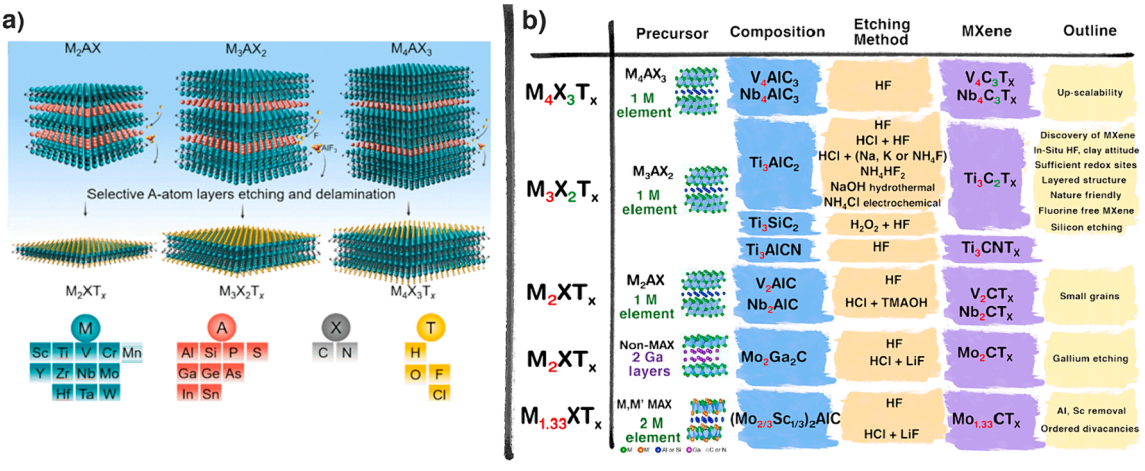

Fig. 3. (a) Schematic illustration of MAX precursors for the synthesis of MXenes via selective etching. Reproduced with permission from Ref. [104] Copyright 2021, Wiley. (b) Transformation of MAX to MXenes family reported for different applications.

selective etching out of the A layers. The M, A, and X compositions of the MAX precursor are crucial in determining the methods available to synthesize MXenes. MAX phases also possess resistance to high temperatures or oxidation [113,114].

The structural difference between M_2AX and M_2A_2X is the insertion of an extra A layer in M_2A_2X. The lattice constant between M_2AX and M_2A_2X remains almost unchanged [90,115]. However, due to the extra A layer along z-axis in M_2A_2X, lattice constant c is changed [116]. So far, about 60 M_2AX phases have been synthesized. A few of them (Mo_2GaC [117], Nb_2SnC [118], Nb_2AsC [119], Nb_2SC [120], Ti_2InC [121], Nb_2InC [122], Ti_2InN [123], Ti_2GeC [124], Lu_2SnC [112], and Nb_2GeC [125]), show superconducting properties [125,126]. Being member of double-A-layer MA_2X phases, Mo_2Ga_2C is extensively explored. In the new compound (Mo_2Ga_2C), two Ga layers were formed instead of one in Mo_2GaC and all other MAX phases. In simple description, we can think a mere insertion of an extra Ga layer on top of the existing Ga in to Mo_2GaC (2 1 1) so that the new phase Mo_2Ga_2C (2 2 1) is formed. Moreover, due to the similarity of electronic bonding, elastic properties and structure with superconducting Mo_2GaC, Mo_2Ga_2C might also have similar superconducting, thermodynamics and optical properties [127]. Later in the year 2016, another double-A-layer MAX phase was reported by *Fashandi et al.* in three different ternary compounds, i.e. V_2Ga_2C, Ti_2Au_2C and $Ti_3Au_2C_2$ [128].

4.1. Synthesis strategies of TMC MXenes

Traditional MXene synthesis relies heavily on high-temperature synthesis methods, which subject precursor materials to elevated temperatures to form MXenes. However, this conventional approach has inherent limitations that affect MXenes' performance in electro(photo)chemical and photocatalytic applications. High-temperature synthesis leads to larger crystal growth, reducing surface area and active sites available for reactions. This reduction in surface area hampers performance in applications like water splitting, supercapacitors, and batteries, limiting charge storage and energy density. Additionally, in photocatalysis, it reduces the efficiency of photon absorption and catalytic reactions, affecting the material's ability to harness light energy for chemical transformations. As a result, researchers are exploring alternative synthesis methods like Ball-milling, liquid exfoliation, chemical etching, intercalation, hydrothermal/solvothermal treatment, ultra-sonication, microwave irradiation to address these challenges. Hydrothermal/Solvothermal synthesis (Fig. 4a, b) is one of the best approaches to the successful synthesis of Mxenes. This approach involves the use of a solvent and temperature (typically in the range 120 to 200 °C) to synthesize TMC MXenes (for example, the synthesis of $Ti_3C_2T_x$ through the reaction of TiO_2 and hydrocarbon precursors in a solvothermal environment) [129,130]. To date, ultrasonic method which is an eco-friendly and completely safe approach utilized in the production of MXene and MXene quantum dots (QDs). This technique leverages solvents such as DMSO, DMF, N-methyl-2-pyrrolidone (NMP), and tetra-butylammonium hydroxide (TBAOH), each possessing high boiling points and surface energies. Through the application of acoustic energy, cavitation, and reverberation within solvents, ultrasonication effectively converts both layered and non-layered materials into QDs while preserving their inherent

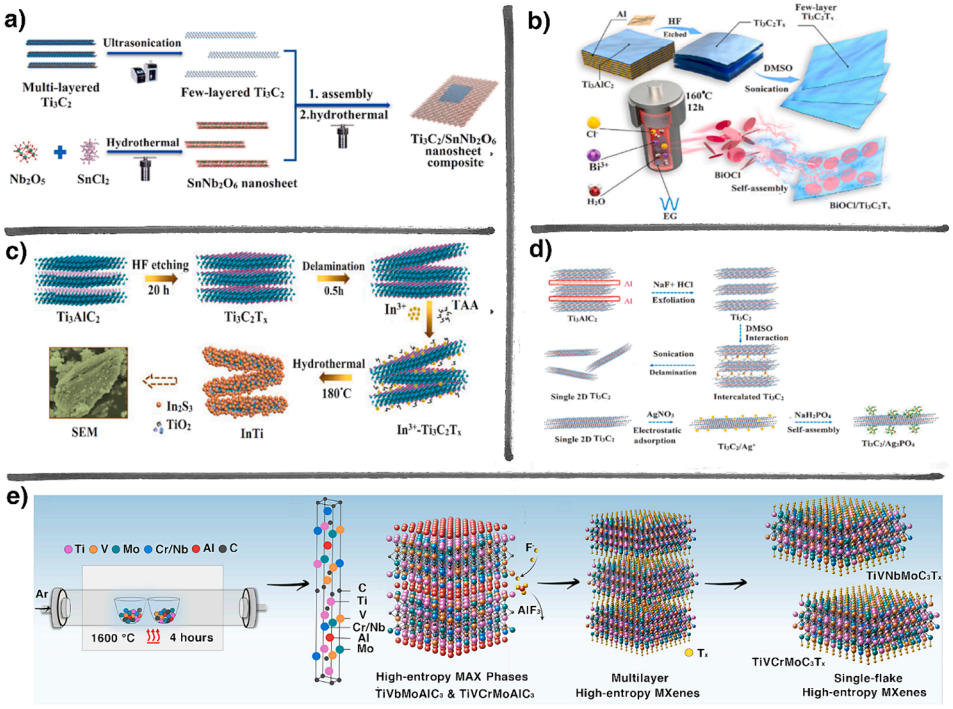

Fig. 4. Schematic illustration of heterostructure preparation procedure (a) $Ti_3C_2/SnNb_2O_6$ (b) $BiOCl/Ti_3C_2T_x$ (c) $In_2S_3/TiO_2/Ti_3C_2$. Reproduced with permission from Ref [136] Copyright 2018 Elsevier (d) Ag_3PO_4/Ti_3C_2. Reproduced with permission from Ref [142] Copyright 2018, Elsevier (e) Synthesis route for high-entropy MXenes. [138] Copyright 2021, American chemical society.

characteristics. Due to the solvents' acoustic, cavitation, and reverberation, the ultrasonication process changes the layered, as well as nonlayered, materials into QDs [131]. TMC MXenes can be synthesized by exfoliating bulk TMC materials, such as Ti_3C_2, using strong acids, like HF, to selectively remove the transition metal layer and leave behind a few layers of the TMC [132]. TMCs can be also synthesized via electrochemical etching. This process involves electrochemical etching of bulk TMC materials, such as $Ti_3C_2T_x$, in an electrolyte solution to obtain TMC MXenes [133]. Thermal annealing is also a substantial synthesis approach to get a pure TMC MXenes by annealing precursors, such as metal oxides or metal nitrides, in a reducing atmosphere to produce the desired TMC [134–136]. However, MXenes are most commonly synthesized through selective etching of A atoms from originally layered MAX (Fig. 4c,d). In the transformation of MAX to MXenes, the etched layers are replaced by the termination groups such as –OH, –O, or –F, to form layered materials consisting of $M_{n+1}X_nT_x$ multilayers interconnected with van der Waals bonds. The termination groups in MXene structures can enable high hydrophilicity of the MXene sheets. Cao *et al*, [137] fabricated sandwiched heterostructures through a two-step self-assembly approach, by which the 2D MXene nanosheets were first assembled onto microbial nanoribbons, and transition metal ions were deposited onto the surfaces of MXene nanosheets to form sandwiched heterostructures owing to the oppositely charged ions and $Ti_3C_2T_x$ nanosheets. Since 2004, MXenes have also emerged as a promising precursor for multi-principal-element (MPE) high-entropy alloys in bulk 3D crystalline compounds and high entropy 2D carbides. The high-entropy metal alloy concept is a materials synthesis strategy where several (usually five or more) elements are combined in high and near equiatomic concentrations (5–35 at. %) to stabilize a single-phase formation, instead of multiphases of solid solutions with different compositions and crystal structures. MXenes allows new elemental combinations and introduction of elements previously not used for MAX phases to transform MXenes to high-entropy MXenes. Inspired by the two fast-growing fields of high-entropy compounds and 2D MXenes, *Srinivasa et al*, [138] reported on successful development of $TiVNbMoAlC_3$, $TiVCrMoAlC_3$, $TiVNbMoC_3T_x$ and $TiVCrMoC_3T_x$ high-entropy alloys by using MAX materials as precursor (Fig. 4e). The development of high entropy alloys confirms the importance of configurational entropy in stabilizing the desired single-phase high-entropy MAX over multiphases of MAX, which is essential for the synthesis of phase-pure high entropy MXenes [139–141]. The synthesis of high-entropy MXenes significantly expands the compositional variety of the MXene family to further tune their properties, including electronic, magnetic, electrochemical, catalytic, high temperature stability, and mechanical behavior.

Particularly, the different synthesis routes for a specific type of MXenes can influence the physicochemical properties of the obtained MXenes and their related applications. According to previous reports, the hierarchical MXene/TMD hetero structures are always synthesized through a two-step synthesis strategy including the synthesis of MXenes and subsequent growth of TMC structures on MXenes. In general, the synthesis methods of MXenes can be classified into HF selective etching (Fig. 5a) (Mo_2ScAlC_2 to Mo_2ScC_2 and Mo_2TiAlC_2 to Mo_2TiC_2), followed by ultrasonic delamination (Fig. 5b) [100,143–145]. Nowadays, the corresponding theory, production, identification, manipulation, and application of these 2D materials have been rapidly expanded and further developed. Typically, the following different MXenes like V_2CT_x [146], $V_4C_3T_x$ [147], Nb_2CT_x [148], $Nb_4C_3T_x$ [149], $Ta_4C_3T_x$ [150], Ti_2NT_x [151], Ti_3CNT_x [150], Ti_2CT_x [152], $Mo_{1.33}CT_x$ [153], and $Mo_2TiC_2T_x$ [100] are fabricated via etching synthesis method. Recently, new synthesis methods were developed, such as the combination of an aqueous HF and HCl (HF/HCl) synthesis called wet-chemical etching (Fig. 5i) [154,155], non-aqueous wet-chemical etching process using NH_4HF_2 (Fig. 5ii), [133] and molten salt etching (Fig. 5iii) [104,156,157]. HF/HCl etching of MXene can be used to control the amount of HF necessary for the exfoliation process, which has shown to result in a lower defect density and improved electrical properties [158]. Non-aqueous etching of MXene permits dispersion of MXene flakes in solvents other than water, for which long-term storage of MXene in water has shown an overall decrease in electrical conductivity due to oxidation of MXene sheets [159]. These synthesis strategies can produce TMC MXenes with different

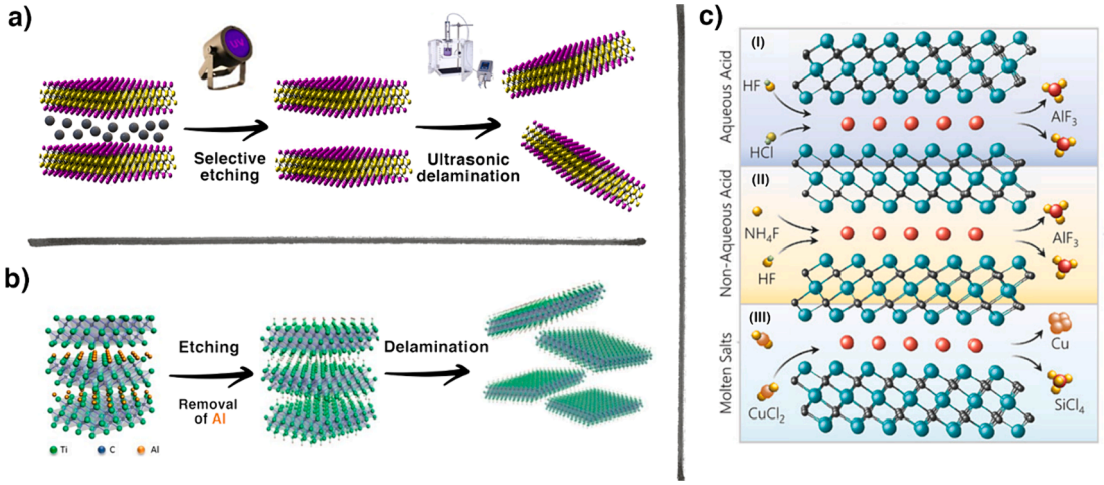

Fig. 5. Schematic illustration of (a) $(Mo_{2/3}Sc_{1/3})_2AlC$ before etching, after etching and delamination. (b) UV based selective etching and ultrasonic delamination. (c) MXene synthesis routes (i) aqueous etching (ii) non-aqueous etching and (iii) molten salt etching. Reproduced with permission from Ref. [104] Copyright 2021, Wiley.

properties, depending on the conditions and precursors used. Further, the choice of synthesis strategy depends on the desired end use application of the TMC MXene material.

4.2. TMDs-TMC MXenes hetero-structures

Overcoming the limitations of TMDs [58,160] and MXenes [161,162] for large-scale applications has become a pressing concern. To address these challenges effectively, the utilization of heterostructures emerges as the most promising approach. Designing new materials at lower dimensionality has been proven to be a successful approach to achieve new paradigm shift in catalysis. Unusual properties and phenomena can be realized by stacking 2D materials of different properties including TMCs-TMDs ($W_xC@WS_2$ [163], WSe_2/SnS_2 supper lattice) TMDs-LDH (MoS_2/NiFe-LDH supper lattice), LDH- metal oxides [6,7,164], TMDCs-2D layered materials (MoS_2/G super-lattice) TMDs–MXene (MoS_2, WS_2, and $MoSe_2$ /Ti_2CT_2) into vdW hetero-structured. *Gogotsi et al*, [165] employed concentrated HF acid based synthesis approach for the targeted etching of the Al layers within the Mo_2TiAlC phase. Subsequently, the resulting multilayer $Mo_2TiC_2T_x$ material was subjected to sonication under an Ar flow, as illustrated in Fig. 6a. Furthermore, different synthesis approaches (acid etching, hydrothermal and magnetic hydrothermal approach, as summarized in Fig. 6b) have been developed for the successful synthesis of heterostructured materials [166]. These heterostructures combine the advantages of the individual components to overcome certain limitations. A good example is the utilization of graphene's excellent electrical conductivity, and high surface area [165], with the chemical versatility of TMDCs to unlock new applications in energy storage (Li ion, Zn ion, Na ion batteries) and conversion (water splitting) [137,167]. Moreover, MXenes with layered structure can provide a stable conductive network and relieve the huge volume change of TMCs in the heterostructure [168]. 2D hetero-structures, made by stacking different 2D crystals scaffolds have attracted great attention for energy storage applications. [169] In heterostructured materials [7,164,170–173], the intimate interfacial interaction between 2D materials affects the conductivity that facilitate ionic and electronic transport, which improves the electrochemical performances [174–177]. Therefore, forming hetero-structure between the 2D materials brought synergetic benefit from the individual components and expanded the utilization of the materials in energy storage and conversion (Fig. 6c). In fact, compared with the single-component catalysts, the hetero-interface catalysts have several advantages including the electronic interactions between different components, and the synergistic effects. Most importantly, developing routes for the synthesis of structures with more active sites in the basal plane is also remaining a significant challenge [177]. C. Chen et al. have presented findings on a heterostructured material formed between MoS_2 and $Mo_2TiC_2T_x$. In the designed material, MoS_2/$Mo_2TiC_2T_x$ exhibited initial charge and discharge capacities of 554 and 646 mA h g^{-1}, respectively, at 100 mA g^{-1}. These values are 4.1 and 2.4 times higher than those of pure $Mo_2TiC_2T_x$ (134 and 268 mA h g^{-1}, respectively). The observed increase in capacity is aligned with the much higher theoretical capacity of 670 mA h g^{-1} for MoS_2-MXene. attributed to the open structure of $MoS_2/Mo_2TiC_2T_x$, in contrast to the restacked pure $Mo_2TiC_2T_x$. This work demonstrates the feasibility of constructing MXene-based 2D heterostructures for electrode materials in energy storage and conversion, opening new possibilities for various applications. In essence, the study lays the

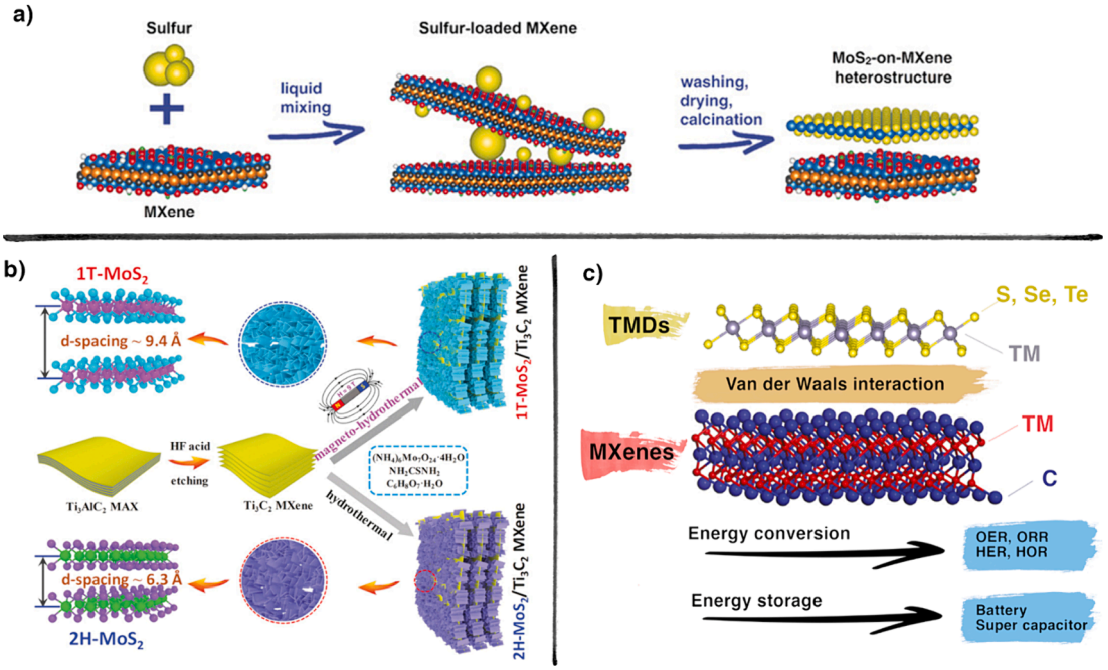

Fig. 6. Schematic representation for the preparation of (a) MoS_2/MXene hybrids. Reproduced with permission from Ref [165] Copyright 2018, Wiley. (b) 1 T-MoS_2/Ti_3C_2 MXene and 2H-MoS_2/Ti_3C_2 MXene 3D hetero-structures[166] Copyright 2020, Wiley (c) TMD/MXene hetero-structure for energy storage and conversion Application.

foundation for utilizing MXene in the development of 2D heterostructures for energy storage applications [165]. P. K. L. Tranan and coworkers [178] have reported the utilization of an interfacial engineering approach to explore a novel hybrid structure comprising a two-dimensional cobalt sulfide-Mxene (2D CoS-Mo_2TiC_2) heterostructure supported by a three-dimensional foam substrate. The distinctive interfacial interactions induced a noteworthy augmentation in the number of electroactive sites and enhanced charge transfer ability, thereby expediting the kinetics of both HER and OER in an alkaline medium. The catalyst exhibited overpotentials of 248.2 mV and 310 mV at a current response of 50 mA cm^{-2} for HER and OER, respectively, coupled with notable stability. Furthermore, a two-electrode electrolyzer fabricated using the developed 2D CoS-Mo_2TiC_2 catalyst demonstrated a cell voltage of 1.74 V at 10 mA cm^{-2}, exhibiting commendable stability over 25 h of continuous operation. These outcomes were attributed to the formation of a distinctive interfacial heterostructure, characterized by robust interactions between the two material phases, effectively modifying the electronic structure and surface chemistry, thereby enhancing catalytic performance.

Furthermore, recent studies show introduction of nano-carbon, conductive polymers, heteroatoms, and metal oxides are also other approaches that solve the issues and challenges in TMC MXenes and TMDs. Further, the increase of interlayer distance in TMDs was also investigated to yield better electrochemical performance [179]. For a heterostructure, several features, like the lattice mismatch, stacking order, component layers, and so on, can affect its electronic structure. Hence, TMD/MXene heterostructure proven satisfactory reverse capacitance at high current rates, outstanding durable performance, specific capacitance, enhanced coulombic efficiency, and enhanced ion transport and structural stability during redox reactions [163,180,181]. Based on these outstanding results, heterostructure formation between the 2D structures of MXenes and TMDs is a substantial approach to solve the issues and challenges in TMC MXenes and TMDs. Heterostructure formation between the two materials avoids the restacking in TMCs. For this reason, synergetic interaction between the different material phases is generally expected [182–185] and the heterointerface consists of vdW interactions that can prevent Fermi level pinning [186]. The various advantages of TMDs over other 2D layered materials (see in section 2) have spurred a diverse array of applications, including their use in processes such as water splitting (HER and OER), fuel cells (HOR and ORR), CO_2 reduction (CO_2RR), nitrogen reduction (NRR), as well as in Li-ion and Li-S batteries. Nonetheless, TMDs face common challenges and bottlenecks that compel researchers to focus on achieving precise geometrical alignment between different layers in heterostructures, as this alignment plays a fundamental role in tuning the electronic structure [187,188]. In this context, it is crucial to create heterostructures by integrating TMDs and Mxenes through a process involving selective acid etching, hydrothermal and CVD treatments of TMC MXenes and TMDs. Subsequently, delamination and exfoliation need to be employed hence modifying the

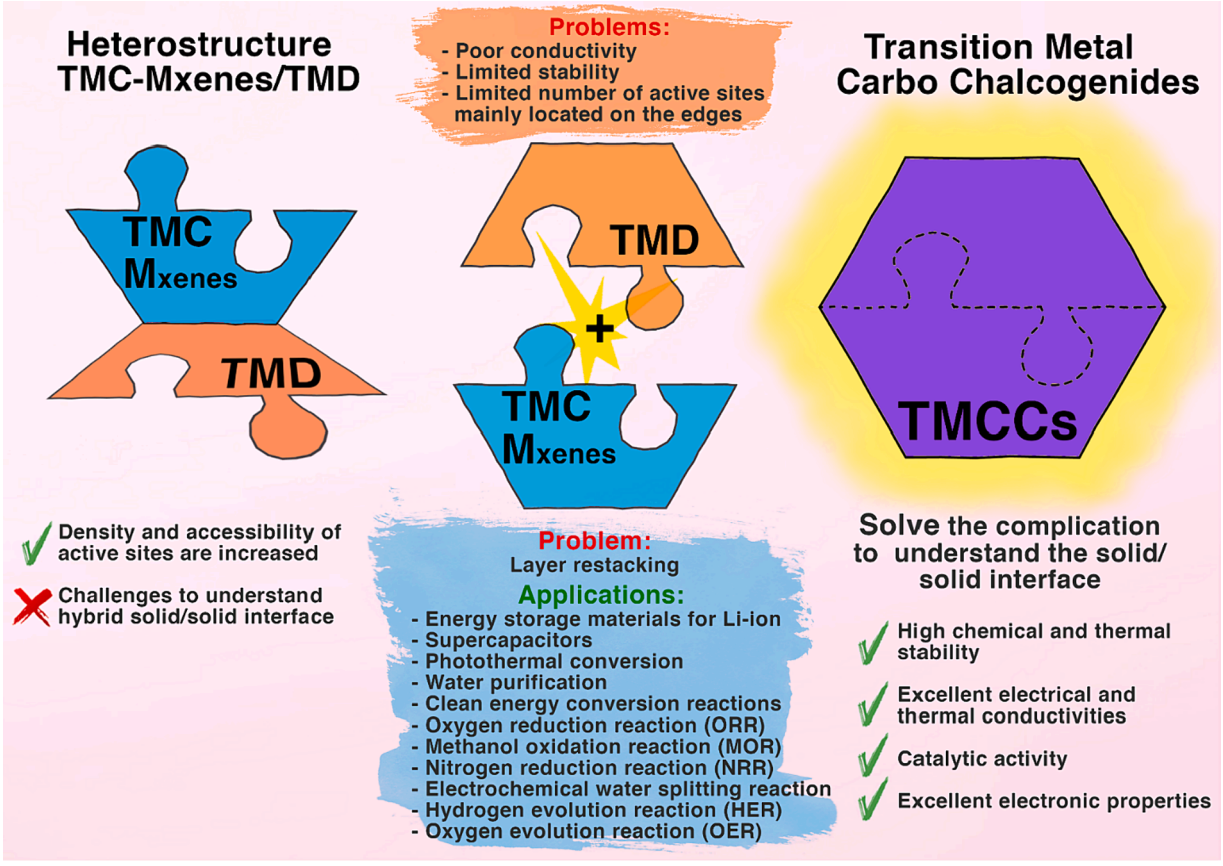

Fig. 7. Key features, merits, and open issues of the 2D TMC MXenes, TMDs, their heterostructure and the new layered TMCCs materials with their potential application.

surface area, enhancing their properties. As a result, different research's confirms that, TMC MXene-TMD composites demonstrated excellent activity, stability in electrocatalysis and with superior reversible specific capacitance, columbic efficiency, improved cyclability and rate performance in battery [137,189]. There are several review papers regarding the design of TMC MXenes/TMDs heterostructure [190,191]. The aim of this review is not about this kind of heterostructure. Thus, interested readers are suggested to refer to comprehensive reviews on the topic. An intriguing aspect that warrants attention at this juncture is that all the advantages associated with heterostructures can be found within a single integrated framework, namely TMCCs. This emerging family of 2D materials possesses immense potential across various applications, making a timely exploration of this subject invaluable to researchers in related fields.

5. Frontier in transition metal carbo-chalcogenides (TMCCs)

The challenges encountered in the restacking of MXene layers and TMDs for electrochemical energy conversion and storage arise from their inherent limitations in electrical conductivity and stability [174,192]. TMCs, a significant framework in MXenes, have emerged as a distinct class of materials with exceptional electrical conductivity that surpasses that of TMDs. These carbides exhibit metallic behavior and possess highly conductive pathways for charge transport, making them attractive candidates for various electrochemical applications. The high conductivity of TMCs is a result of their delocalized electronic structure and the presence of metallic bonds, which enables efficient movement of charge carriers.

The remarkable contrast in electrical conductivity between TMCs and TMDs has motivated researchers to explore a groundbreaking strategy: integrating these two material families into a unified system. This integration aims to eliminate the need for interfaces that can introduce complications and hinder performance, like the challenges encountered when stacking Lego building blocks. By merging TMDs and TMCs without interfaces, researchers can create a seamless material that capitalizes on the unique advantages offered by each component. This approach enables improved charge transport throughout the structure, facilitated by the highly conductive TMCs, ultimately enhancing the overall electrochemical performance. Furthermore, this merging approach offers additional advantages beyond improved electrical conductivity. It simplifies the understanding of solid/solid interfaces, which can be intricate and challenging to characterize. By consolidating the two material families, researchers can focus on optimizing the composition and structure of the unified material without the complications introduced by the interfaces. By harnessing the unique properties of TMCs and merging them with TMDs, researchers are unlocking exciting opportunities for the creation of innovative materials that can revolutionize the field and pave the way for sustainable and efficient energy systems. The resulting merged materials, known as TMCC, Fig. 7, hold tremendous potential as novel candidates for structural materials in various application fields. This newly expanding 2D layered carbo-chalcogenides materials are also named as transition metal carbo-sulfide [193,194]. Notable group of layered materials is the layered transition metal carbo-chalcogenides (TMCCs), including compounds such as Nb_2S_2C [195], Nb_2Se_2C [196,197], Ta_2S_2C [198], and Ta_2Se_2C [199]. These materials can be seen as a fusion of two well-established families of materials, namely transition-metal carbides (MXenes) and TMDCs. The vdW interaction between the terminated sulfur (S) layers in bulk TMCCs allows for the formation of highly crystalline 2D TMCCs. However, despite their potential, these materials have been largely overlooked by the 2D materials research community. The M-C bond in TMCCs exhibit not only enhanced electrical conductivity but also exceptional thermal and chemical stability, making them highly desirable for demanding operating conditions [200]. Additionally, certain TMCC compositions have demonstrated superconductive properties, opening possibilities for novel applications in quantum technologies and beyond.

TMCCs represent a new frontier in material design, particularly for electrochemical energy storage and conversion applications. These materials have received significant attention in recent years due to their unique electronic, optical, and catalytic properties, making them promising candidates for a wide range of applications. For example, some TMCC families, such as Nb_2CS, Nb_2CSe, Ta_2CS, and Ta_2CSe, have exhibited high-temperature superconductivity, suggesting potential use in superconducting electronics. TMCCs hold promise in the creation of highly effective electrocatalysts for processes like oxygen evolution. Despite their significant potential, there

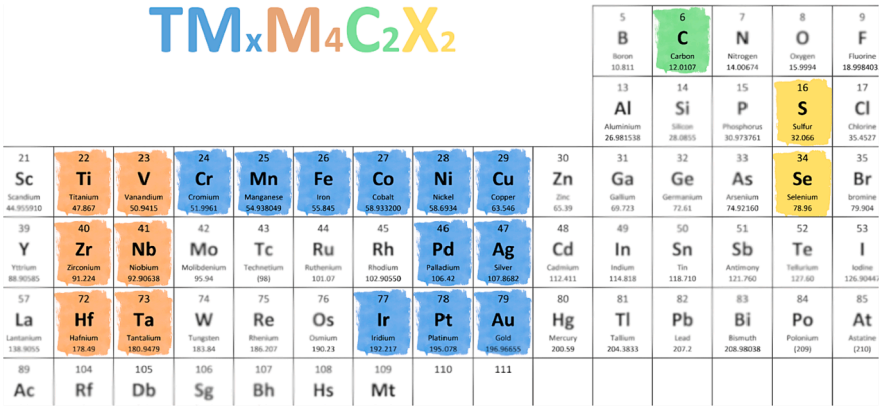

Fig. 8. Elements that can form thermodynamically stable TMCCs (M) and possibly intercalating metals ions (TM).

is still a considerable amount to be uncovered and comprehended regarding these materials. Their unique electronic structure and bonding characteristics, influenced by the interplay between metals (such as Ti, Nb, Ta), S, Se, and C, make them a rich and complex class of materials that are not fully comprehended. The presence of multiple light elements in close proximity, such as C and S, introduces challenges during the analysis and characterization of TMCCs [201]. In addition, designing single-component crystals from the merging of two different crystals offers advantages in terms of understanding the mechanism, comprehending the properties, and enabling easy scalability. TMCCs, with their atomic-level thickness, enlarge the specific surface area, expose more active sites, and enhance intrinsic catalytic activity. However, the successful synthesis of TMCCs is currently limited to certain transition metal carbides, such as Ti, Zr, Hf, and Nb, due to the thermodynamic instability of other transition metal carbides (Fig. 8). [202,203].

TMCCs exhibit two distinct phases: the H-phase and the vdW-type carbo-sulfide phase [204]. The H-phase has a composition of M_2SC, where M represents transition metals such as Ti, Zr, or Nb (for example, Hf_2FeC_2S). This phase consists of layers with the fundamental structure S-TM-C-TM-S, where TM refers to the transition metal. The layers in the H-phase are connected to each other through weak vdW forces. On the other hand, the vdW-type carbo-sulfide phase is represented by the formula TM_2S_2C, where M can be Nb or Ta (e.g., Ta_2S_2C, Nb_2S_2C). In this phase, the fundamental layers of S-TM-C-TM-S are also present, but they are linked through vdW forces. These vdW forces are relatively weak, allowing for easy sliding between the layers. However, carbo-sulfides with the formula TM_2SC (where TM represents Ti, Zr, Hf, or Nb) are not layered compounds and lack the weak vdW bonding between the sulfur atoms. These compounds are highly stable and relatively hard [205].

The TMCCs containing TMDs and MXenes have a fundamental layer structure of S-TM-C-TM-S. The Nb_2S_2C monolayer, for example, exhibits good kinetic and thermodynamic stability and possesses metallic properties with significant electronic states at the Fermi level [120]. The superconducting nature of TMCCs mainly arises from the M-C layers, while the MS_2-type structure contributes to the Anderson localization effect. It is important to note that TMCCs represented as TM_2S_2C (M = Nb, Ta) have a different structure compared to MAX phases. In TM_2S_2C phases, two different sulfur layers are stacked between the carbide layers. This large family of 2D TMCC materials has gained recent attention and shows great promise, particularly in the field of electrochemical energy. Despite their potential, TMCCs have seen limited applied research, which can be attributed to the challenges involved in their synthesis [206]. The difficulty in synthesizing these compounds has been a significant hurdle in their exploration and utilization. Overall, TMCCs with their unique layered structures and properties hold great potential for a range of technological applications, and ongoing research aims to further understand their synthesis, properties, and potential uses.

5.1. Structure and chemistry of the M_2C_2S and M_2CS phases

The new families of TMCCs exhibit diverse formulas like TM_2SC, $TM_4S_2C_2$, or TM_2S_2C, resulting in distinct physical and chemical properties [207]. Some notable members, such as Ta_2S_2C and Nb2S2C, were discovered in the 1970s [208]. These compounds have layered structures in their 3R phases, with sulfur layers between carbide layers. Two prototypes of Ta_2S_2C, low-temperature (1s) and high-temperature (3s) modifications, were identified. Nb_2S_2C also has both 1s and 3s structures, where the latter is stable at high temperatures. Intercalation of transition metal atoms can stabilize these modifications. Though Nb_2Se_2C and Ta_2Se_2C exist, they have been overlooked in the 2D materials field [209,210]. Ti_2SC is another unique compound with potential applications due to its distinctive mechanical properties. TMCCs exhibit superconductivity at 7.55 K, but research on Ti_2SC is hampered by challenges in obtaining high-purity samples. TM_4S_2C carbo-sulfides, like Ti_2SC, are robust compounds with chemical stability similar to corresponding carbides [201].

5.1.1. Structure and chemistry of the $TM_4C_2S_2$ phase

It is widely recognized that sulfur-containing phases exist in $TM_4C_2S_2$, and yet surprisingly little has been published on their chemistry, origin, and effects on the mechanical properties of these 2D materials. The $TM_4C_2S_2$ class of materials are a common constituent of transition metal bearing steels, where it has been implicated in the process of fracture. They possess a hexagonal structure of D^4_{6h}-P63/mmc space group with lattice parameters $a_0 = 3.21$ Å and $c_0 = 11.20$ Å when M = Ti, and $a_0 = 3.395$ Å and $c_0 = 12.11$ Å when M = Zr. $Ti_4C_2S_2$ have similarity in the diffraction patterns with γ-Ti_2S [120]. The thermodynamic formation energy of $Ti_4C_2S_2$ was originally specified as $\Delta^oTi_4C_2S_2$ = -1994.5 + 0.231TkJ/mol). This family of 2D materials are formed when sulfur segregates to grain boundaries during very high temperature treatment, which leads to the formation of the sulfo-carbides when melting is involved. The identification of carbo-sulfides was based on X-ray powder-diffraction and electron-microprobe analysis. However, no quantitative microprobe data was obtained, and no carbon was detected, thus leaving the chemistry of these particles uncertain. It was demonstrated that differential thermal analysis evolved gas analysis (DTA – EGA) is the best method for discriminating between γ-Ti_2S and $Ti_4C_2S_2$ [211]. However, misidentification is common when microscope, microprobe and particularly X-ray diffraction procedures are used, because the diffraction patterns of γ-Ti_2S and $Ti_4C_2S_2$ are similar.

5.1.2. Intercalation and delamination chemistry of $TM_xM_xS_xC$ materials

The synthesis of homogeneous compounds becomes increasingly difficult as the number of elements involved increases, mainly because of the greater availability of reaction paths. As a result, more stable compounds are formed first, which can act as diffusion barriers. Intercalation and delamination processes are necessary to obtain single-layer TMDs nanosheets [212]. Compared to stacked TMCCs, single-layer TMCCs nanosheets exhibit superior chemical properties, such as high specific surface area, good hydrophilicity, and rich surface chemistry. To further enhance the superconducting properties of TM_2S_2C materials, temperature, and intercalation of a wide range of guest elements are crucial. Superconductivity in 2D materials is a recent and attention seeking area in condensed matter physics [213,214]. 2D materials, composed of TM, C, and S atoms have displayed superconducting properties in the past few

decades, prompting extensive research. TMCCs are prized for their tunable properties, allowing scientists to control parameters such as the superconducting transition temperature. They can exist in both 2D and 3D structures, with 2D variants often exhibiting unique quantum effects and higher Tc values. While the exact superconductivity mechanism varies, it typically involves the formation of Cooper pairs. Cooper pairs showed that an arbitrarily small attraction between electrons in a metal can cause a paired state of electrons to have a lower energy than the Fermi energy, which implies that the pair is bound [215]. In conventional superconductors, this attraction is due to the electron–phonon interaction which is responsible for superconductivity [216]. TMCCs hold promise for applications in quantum computing, superconducting electronics, and potential use as high-temperature superconductors. However, challenges remain, such as developing stable synthesis methods, and ongoing research seeks to enhance their practicality and understanding. During the intercalation of metal ions into the vdW gaps of TM_2S_2C, the type of metal used determines the interlayer spacing. Alkali metals, such as Li, occupy all vdW gaps, thus increasing the interlayer spacing. According to the ionicity diagram, Li derivative intercalation falls within the octahedral domain, whereas K, Rb, and Cs compounds are in the trigonal prismatic region, and Na is a borderline case with both an octahedral and trigonal prismatic phase.

Boller et al. reported intercalate phases of transition metals (TM = Ti, V, Cr, Mn, Fe, Co, Ni, Cu) to the layers of Ta_2S_2C to form $Ti_x[Ta_2S_2C]$, $Cu_x[Ta_2S_2C]$, $Fe_x[Ta_2S_2C]$, $Co_x[Ta_2S_2C]$, and $Ni_x[Ta_2S_2C]$ [195,207,217]. Intercalating elements, such as Ti, Cr, Mn, Fe, Co, and Ni, occupy the octahedral voids in the sulfur double layers, while Cu is intercalated into the tetrahedral sites between sulfur and tantalum layers in TM_2S_2C [204]. Metals like, Fe, Co, Ni, or Mn can introduce magnetic properties into TMCCs, making them useful for magnetic data storage or magnetic sensing. The intercalation of Li^+, Na^+, and K^+ increases the interlayer spacing in TMCCs sheets and improves their electrochemical properties, making them suitable for use in Li-ion or Na-ion batteries. The structural variation is caused by different electronic effects in the interaction between host and guest. Most of the transition metal intercalation results in a metastable compound except V, yet by substituting Ti for V, $V_{0.6}Ti_{0.42}SC$ can be synthesized. To confirm the structural differences between intercalated and pristine materials, *Walter et al.,* studied XPS core level spectra and valence band region using XPS as illustrated in Fig. 9 [217]. The results show that metal intercalation ions (Fe, Co, Ni or Cu) cause a shift in 1s C, Ta(4f) and S(2p) XPS core level spectra towards higher binding energies for their core level spectra compared to the pristine material (see Fig. 9a-c). However, as depicted in Fig. 9d the Fe, Co, or Ni intercalated into Ta_2S_2C shows a shift to higher binding energies in the valence band XPS spectra, whereas Cu intercalation shows a shift towards the Fermi edge compared to the pristine Ta_2S_2C [217]. This is because Fe, Co, and Ni are intercalated in octahedral sites between two adjacent sulfur layers, but Cu is intercalated in tetragonal sites between

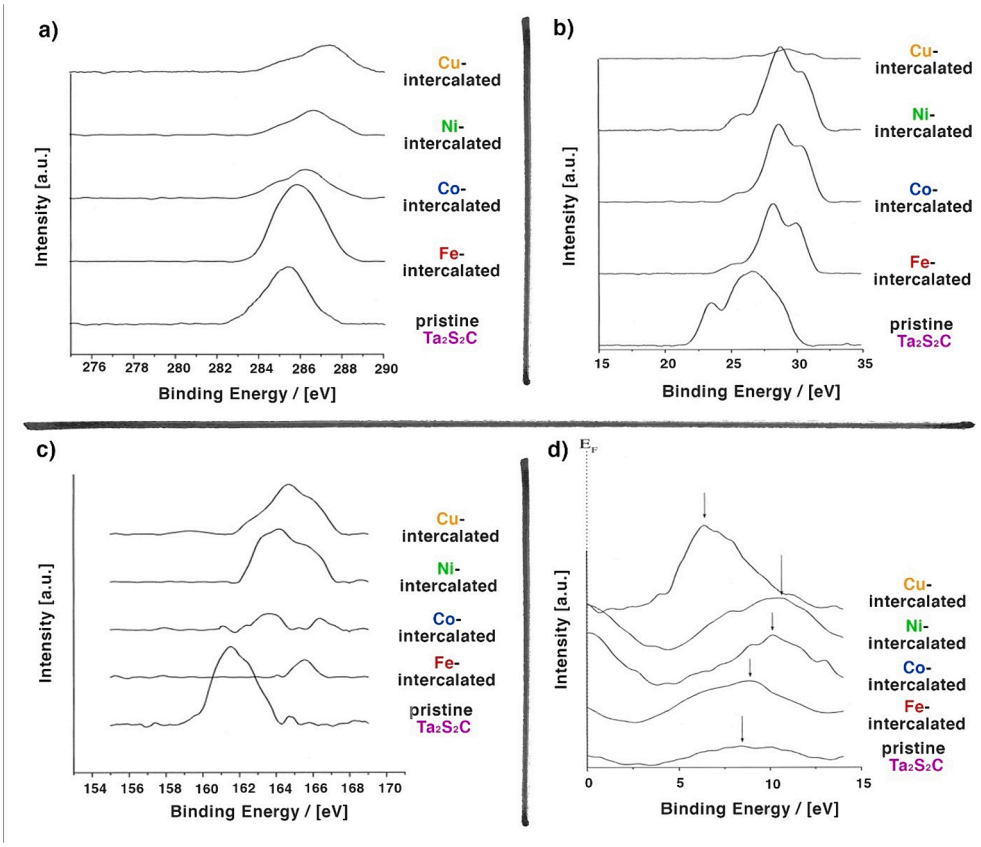

Fig. 9. XPS core level spectra of pristine and intercalated Ta_2S_2C (a) 1s C (b) Ta(4f) (c) S(2p) and (d) Valence band XPS spectra of pristine and intercalated Ta_2S_2C. Reproduced with permission from Ref [217] Copyright 2000, Elsevier.

sulfur and tantalum layers [217].

The interlayer distance in the vdWs gap of the Nb_2S_2C host lattice in 1T-$Cu_{0.7}[Nb_2S_2C]$ is 0.5 Å larger than in the 3R-phases. In order to get a meta stable phase of the Nb_2S_2C or Ta_2S_2C, de-intercalation of the metal is mandatory [218]. De-intercalation can be done by two-step treatment of $TM_x[Nb_2S_2C]$ either with iodine in acetonitrile or with concentrated hydrochloric acid. Thus, the deintercalation brought a dramatic decrease of the c axis (Table 1) indicating stacking disorder. In materials which have larger vdW gap like Nb_2S_2C, the metastable host lattice can be isolated by soft chemical deintercalation. To the best of our knowledge, there have been no previous reports of successful exfoliation of TMCCs into single layers. Achieving 2D layers of TMCCs that combine the chemistry of TMDCs (which offer high catalytic activity) while preserving a mechanically robust and metallically conductor carbide core will allow for new property combinations and applications not achievable by TMDCs or carbides alone. However, compared to Ta_2S_2C, there is no simple explanation of the completely different intercalation behavior of Ta_2Se_2C. Noticeably its reduction potential is too negative. Qualitatively the reduction potentials for the reaction $[T_2X_2C] + ne^- \rightarrow [T_2X_2C]^{n-}$ become more negative in the sequence $Nb_2S_2C > Ta_2S_2C \gg Ta_2Se_2C$. From this we can understand that, with respect to their intercalation chemistry, the Nb_2S_2C and Ta_2S_2C are related to 1T-TaS_2, while Ta_2Se_2C resembles more MoS_2, yet without its lubricating properties.

5.2. Properties and structure of TMCC compounds

TMCCs are a class of a new family of 2D materials that exhibit a variety of interesting properties, including electrical conductivity, catalytic activity, magnetic properties, optical properties, mechanical properties, and chemical stability. TMCCs are generally good conductors of electricity, with some exhibiting superconductivity at low temperatures. They are often used as catalysts in various chemical reactions due to their unique electronic and structural properties. Many TMCCs exhibit magnetic behavior, which can be tuned by changing the composition or structure of the material. TMCCs also exhibit interesting optical properties, such as photoluminescence and photoconductivity, making them useful in optoelectronic applications. They are generally strong and rigid materials, making them useful in applications that require high mechanical strength [219]. As well, TMCCs are generally stable under a wide range of chemical conditions, which makes them suitable for use in harsh environments. Composition, crystal structure, and surface functionalization are some of the very important governing factors for electronic properties of TMCCs. To realize the motive behind the metallic nature of the TMCCs (Tm_2S_2C, TM = Nb, Ta etc), it is necessary to study the structure–property relationship [217].

Table 1
Lattice parameters of TM_x $[Ta_2S_2C]$ and TM_x $[Nb_2S_2C]$ phases.

Metal carbo-chalcogenide	a, Å	c, Å	c/a, Å
3s-Ta_2S_2C	3.276	25.62	7.820
$Ti_{0.3}[Ta_2S_2C]$	3.29	25.79	7.832
$V_{0.25}[Ta_2S_2C]$	3.297	25.63	7.772
$Cr_{0.3}[Ta_2S_2C]$	3.293	25.48	7.736
$Mn_{0.33}[Ta_2S_2C]$	3.286	26.30	8.002
$Fe_{0.33}[Ta_2S_2C]$	3.290	25.80	7.839
$Co_{0.33}[Ta_2S_2C]$	3.297	25.24	7.655
$Ni_{0.25}[Ta_2S_2C]$	3.286	25.33	7.708
$Cu_{0.6}[Ta_2S_2C]$	3.290	8.940	2.717
3s-Ta_2S_2C	3.265	8.337	2.615
3s-Nb_2S_2C	3.284	8.56	2.618
$V_{0.6}[Nb_2S_2C]$	3.294	25.76	7.820
$Cr_{0.6}[Nb_2S_2C]$	3.306	25.62	7.749
$Mn_{0.5}[Nb_2S_2C]$	3.306	25.97	7.855
$Fe_{0.5}[Nb_2S_2C]$	3.303	25.83	7.820
$Co_{0.5}[Nb_2S_2C]$	3.305	25.11	7.598
$Ni_{0.5}[Nb_2S_2C]$	3.303	25.33	7.669
$Cu_{0.7}[Nb_2S_2C]$	3.310	9.03	2.728
3s-Nb_2S_2C	3.29	8.94	2.717
1s- Ta_2S_2C	3.265	8.537	2.615
3s- Ta_2S_2C	3.276	25.62	7.821
$Li_1[Ta_2S_2C]$	3.302	26.63	8.065
$Na_{0.15}[Ta_2S_2C]$	3.270	19.50	5.963
$Na_{0.8}[Ta_2S_2C]$	3.302	19.35	5.860
$Na_{0.85}[Ta_2S_2C]$	3.327	19.30	5.801
$Na_1[Ta_2S_2C]$	3.330	19.35	5.810
$K_{0.12}[Ta_2S_2C]$	3.265	31.56	9.666
$K_{0.86}[Ta_2S_2C]$	3.299	31.05	9.412
$Rb_{0.12}[Ta_2S_2C]$	3.280	21.90	6.677
$Rb_{0.86}[Ta_2S_2C]$	3.320	21.45	6.461
$Cs_{0.12}[Ta_2S_2C]$	3.285	22.68	6.904
$Cs_{0.86}[Ta_2S_2C]$	3.315	22.17	6.688

However, there is limited research (both experimental and theoretical study) to understand the structure–property relationship [220]. Generous efforts need to understand the fundamental mechanism by theoretical models, via supporting with experimental findings. However, most of theoretical calculations in literature used ground-state DFT with less consideration of the solvent effects, the impacts from solvated ions, or the transition states of elementary reactions. Recent research pointed out the explicit solvent model, and theoretical investigations are helpful to provide guidance on material design to the experimentalists.

5.2.1. *Crystal structure*

TMCCs have a unique layered structure in which the transition metal, chalcogenide, and carbon atoms are arranged in a stacked arrangement and in a hexagonal arrangement, respectively. The TM_2CS structure, represented by the elements Nb and Ti, has a hexagonal structure with a space group $P6_3/mmc$, prototype Cr_2AlC and two formula units per unit cell [221]. To determine the crystalline arrangement of Nb_2Se_2C, we utilized Rietveld refinement on the PXRD pattern of the chemically analogous compound Ta_2S_2C [196]. The refined parameters for Ta_2S_2C were found to be a = b = 3.315 Å, c = 8.997 Å, with R1 = 8.86, wR2 = 11.7, and χ^2 = 2.59. The stacking sequence of basal planes in TM_2CS materials is AMXMBMXMA…, where A and B refer to carbon planes, M refers to Ti or Nb, and X refers to S [220]. The X_2Se_2C compounds, where X can be either Ta or Nb, exhibit a hexagonal crystal system with a specific space group number. The atomic positions in this space group are as follows: C (0, 0, 0) and X (0.3333, 0.66667, 0.88089), Se (0.66667, 0.3333, 0.69607) (refer to Fig. 10a). In the crystal structure, the $NbSe_3C_3$ octahedron is formed around a central Nb atom, and similarly for Ta, with three Se elements and three C elements. Additionally, the CX_6 octahedron is created by six X atoms surrounding a central C atom (see Fig. 10a, b). All atoms in the structure are six-fold coordinated, with the carbon atoms octahedrally coordinated by the metal atoms and the sulfur atoms trigonally prismatically coordinated by the metal atoms. The choice of element utilized also exerts an influence on the stability of the crystallographic structures. This is evident from the XRD pattern depicted in Fig. 10 c, d, which validates the successful synthesis of H-Nb_2SC and b-Ta_2S_2C. However, it is important to note that b-Ta_2S_2C exhibits greater thermodynamic stability compared to H-Nb_2SC. As a result, b-Ta_2S_2C can be directly obtained through solid-state synthesis [201].

5.2.2. *Electronic band structure*

The electronic band structure plays a pivotal role in determining the properties and potential applications of 2D TMCCs. These materials exhibit structures influenced by interactions among transition metal components, chalcogenides, and carbon atoms. These interactions lead to the formation of localized or delocalized electronic states, impacting electronic and optical properties. The band structure, representing electronic states in energy and momentum space, significantly influences conductivity, optical absorption, and other relevant properties [200,222,223].

In the context of these newly developed 2D ceramics, their mechanical properties are vital for serving as electrically conductive and mechanically robust reinforcements in composites. H. Baaziz and co-workers report the electronic band structures of Nb_2Se_2C and Ta_2Se_2C by using DFT [200]. Fig. 11a,b reveals a clear overlap between the conduction band and valence band, indicating that Nb_2Se_2C and Ta_2Se_2C exhibit a semimetallic nature with an indirect bandgap of 1.1 eV [222,223]. In comparison to NbS_2 and TaS_2, the electronic bands of Nb_2Se_2C and Ta_2Se_2C are broader and more curved. As a result, Nb_2Se_2C and Ta_2Se_2C demonstrate the lowest effective electron mass and the highest electron mobility. The occupied bands below the Fermi level have a dominant contribution of p-orbitals from carbon atoms. Underneath these bands, a particular feature of the CS monolayer is the second bandgap located ≈3 eV

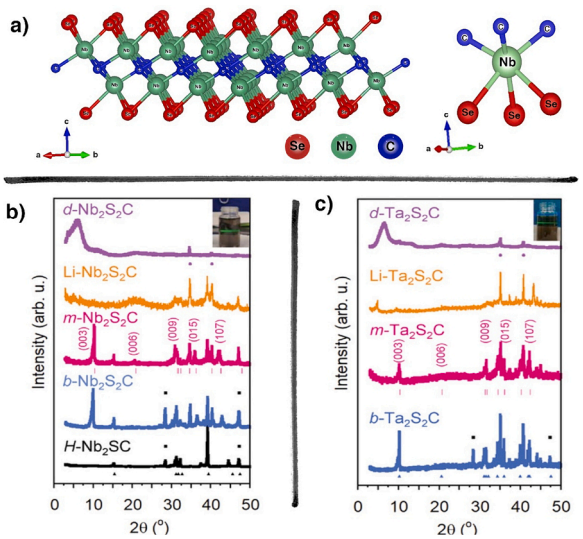

Fig. 10. (a) The crystal structure of the X_2Se_2C compounds. (b) The Nb (Ta) atoms in Nb_2Se_2C and Ta_2Se_2C. Reproduced with permission from Ref [200] Copyright 2023, Springer link. The XRD patterns for (b) d-Nb_2S_2C and (c) d-Ta_2S_2C. Reproduced with permission from Ref [201] Copyright 2022, Wiley.

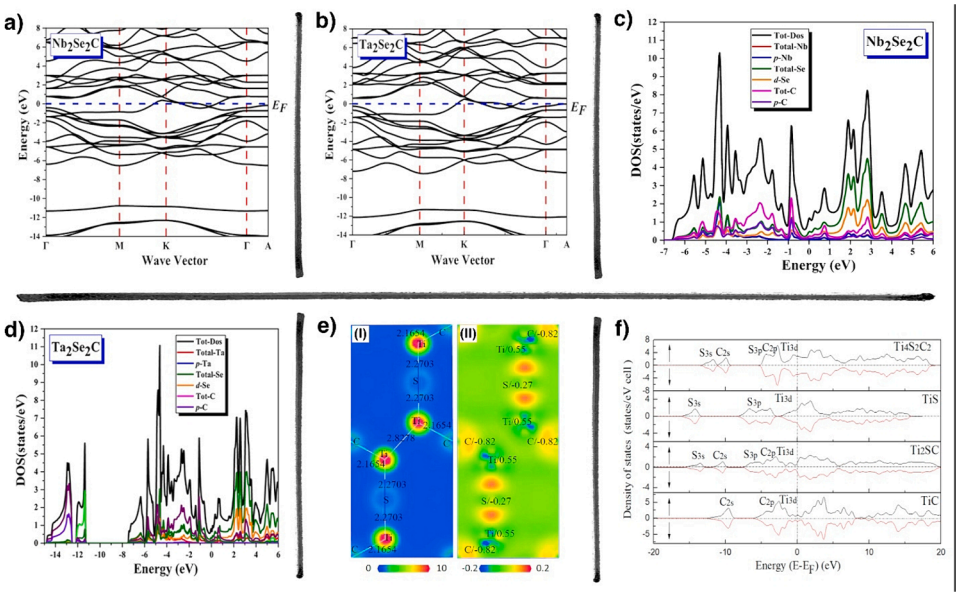

Fig. 11. The band structure of the X_2Se_2C (X = Ta, Nb) compounds. (a) Nb_2Se_2C (b)Ta_2Se_2C.The projected density of state (PDOS) of (c) Nb_2Se_2C (d) Ta_2Se_2C. Reproduced with permission from Ref, [200], Copyright 2023, Springer link. (e) Electron density maps of $Ti_4C_2S_2$ and (i) the bond length (ii) atomic populations (f)The total density of the states for $Ti_4S_2C_2$, Ti_2S_2, Ti_2SC and Ti_4C_4.Reproduced with permission from Ref [225], Copyright 2019, MDPI.

below the Fermi level, followed by bands composed of p-orbitals from sulfur atoms [220,223]. Another report by A. Majed *et al.*, also utilizes DFT, to determine the elastic constants of these 2D TMCCs compared with their TMDs counterparts. The results highlight a substantial improvement in the mechanical stability of Nb_2S_2C (300 GPa) and Ta_2S_2C (319 GPa) when compared to their TMDs counterparts NbS_2 (185 GPa) and TaS_2 (211 GPa), with an enhancement of at least 50 % attributed to the robust TM-C bonding [201]. Strain engineering is also another emerging factor as a potential tool for controlling electronic and thermoelectric responses in carbo-sulfides, although achieving systematic bandgap control remains challenging. Ongoing research explores methods such as doping, stacking orders, and strain to manipulate bandgaps, offering promising avenues for future technologies with unique electronic properties in layered materials [224,225].

The electron distribution and atom-to-atom electron transfer in a compound can be effectively described through the examination of electron density distributions and Mulliken population analysis. As can be seen in Fig. 11e, electron density distribution maps are represented in total electron density and electron density difference maps. The overall electron density distributions for $Ti_4C_2S_2$, Ti_4C_4 and Ti_2S_2 were studied to understand the electron distribution and atom-to-atom electron transfer in a compound. As can be seen from Fig. 11f, the length for Ti–C and Ti–S bonds measures 2.1654 Å and 2.2703 Å in the $Ti_4C_2S_2$. However, the Ti–C bond (2.1659 Å) in Ti_4C_4 in, and Ti–S bond (2.4950 Å) in Ti_2S_2 shows a significant reduction as compared to the Ti–C and Ti–S bonds in $Ti_4C_2S_2$. The Ti_2SC does not spontaneously change into TiS and TiC; however, $Ti_4S_2C_2$ (Z = 2) can spontaneously change into two phases. Conversely, the Ti–C bond length in $Ti_4C_2S_2$ closely resembles that in Ti_4C_4. This suggests that Ti–S bonds experience compression within $Ti_4S_2C_2$ cells, a phenomenon that impairs structural stability for $Ti_4S_2C_2$. Therefore, recently, the M_2SC family of materials are used in practical application as electrocatalyst and battery materials rather than the $Ti_4S_2C_2$ counterpart. [196,201].

D. Zhao and co-workers [225] report a comparative analysis of the electronic structures of Ti_4C_4 (Z = 4), $Ti_4S_2C_2$ (Z = 2), Ti_2SC, and Ti_2S_2 (Z = 2) family of materials on the density of states. Notably, there are no noticeable energy gaps near the Fermi level, indicating the metallic nature of these compounds. As a result, the energy gaps from the lowest valence band to the upper valence band, $Ti_4S_2C_2$ (Z = 2), Ti_2S_2 (Z = 2), Ti_2SC, and Ti_4C_4 (Z = 4) exhibit energy gaps of 3.75 eV, 4.65 eV, 1.98 eV, and 2.37 eV, respectively. This suggests an ionic character in the chemical bonds, with Ti–S exhibiting stronger ionicity than Ti–C. For $Ti_4S_2C_2$ (Z = 2), the sulfur 3 s band predominantly ranges from −13.6 to −11 eV, the carbon 2 s band from −11 to −9.4 eV, and the sulfur 3p and carbon 2p bands from −5.3 to the Fermi level. In Ti_2S_2 (Z = 2), the sulfur 3 s band spans −16.2 to −13.2 eV, and the sulfur 3p band ranges from −8.5 to the Fermi level. Ti_2SC exhibits a sulfur 3 s band between −15.7 and −12.6 eV, a carbon 2 s band from −12 to −9.5 eV, and sulfur 3p and carbon 2p bands spanning from −7.5 eV to the Fermi level. For Ti_4C_4 (Z = 4), the carbon 2 s band extends from −12.7 to −8.5 eV, and the carbon 2p band ranges from −6.1 eV to the Fermi level. A noteworthy observation is the evident shift of the 2 s and 3p energy bands of sulfur to a higher-energy zone for $Ti_4S_2C_2$ (Z = 2), with a more subtle shift in Ti_2SC. Hybridization between S/C p electron bands and Ti 3d electron bands is apparent in these compounds, indicating a covalent interaction between C/S and Ti. Overall, the chemical bonds exhibit ionicity, with Ti–S demonstrating stronger ionicity than Ti–C.

5.2.3. Magnetic properties

TMCCs exhibit magnetic properties that make them favorable for use in magnetic devices. The magnetic properties of TMCCs

depend on the type of intercalating transition metal and temperature. [195,204] The magnetic behaviors of $TM_xTa_2S_2C$ (M = Fe, Co, Ni, Cu) has been determined magnetic susceptibility measurements. At room temperature, all TM_2S_2C samples are paramagnetic. The magnetic properties of $TM_xTa_2S_2C$ M = Fe, Co mainly depend on the magnetic behaviors M^{2+} ions in a crystal field, influenced by the arrangement of atoms in the material as well as by the external factor's temperature and pressure. Thus, $Mn_x[Ta_2S_2C]$ and $Fe_x[Ta_2S_2C]$ have ferromagnetic ordering, whereas $V_x[Ta_2S_2C]$, $Cr_x[Ta_2S_2C]$, $Co_x[Ta_2S_2C]$, and $Cu_x[Ta_2S_2C]$ exhibit anti-ferromagnetic ordering at low temperatures [195,219]. The magnetic susceptibilities of $Cu_{0.7}[Nb_2S_2C]$ are very small and almost temperature independent [207], whereas $Fe_x[Nb_2S_2C]$ samples show a more complex behavior [218,226].

5.3. Synthesis and surface modification approaches

There are several synthesis procedures for TMCCs, including: solid-state synthesis followed by sulfuric acid treatment, [201] CVD, topo-chemical, combustion self-propagating high-temperature combustion synthesis [227,228], mechanical alloying [229,230], molten salt electrolysis [231], chemical/physical exfoliation and hot pressing (HP) method [208], and spark plasma sintering technique (SPS) [232]. HP is a method in which a mixture of precursors is introduced into a reactor and heated to high temperatures, resulting in the formation of TMCCs on a substrate. CVD is commonly used for the synthesis of 2D materials, such as TMCs, TMDs, TMCCs and graphene. SPS is a method in which a mixture of precursors is placed in a die and subjected to high pressure and temperature under an electric current. The resulting TMCCs are formed because of the pressure, temperature, and electric current. Solid-state reaction involves the reaction of metal precursors, chalcogen precursors, and carbon precursors at high temperatures in the solid state. This method is commonly used for the synthesis of bulk TMCCs [208]. 52 years after the first synthesis of bulk TMCCs, 2D Nb_2S_2C and Ta_2S_2C were successfully stripped from parent multilayered Nb_2S_2C using electrochemically assisted exfoliation via intercalation of lithium followed by sonication in water [201]. Additionally, the multilayered Nb_2S_2C has been demonstrated to be a potential superconductor with a T_c of 7.55 K. Therefore, 2D Nb_2S_2C is extremely likely to be another example of intrinsic 2D superconductors exfoliated from layered bulk. In the subsequent sections, we give a brief review of the frequently reported techniques to synthesize TMCCs.

The synthesis approaches mentioned above serve as instrumental tools in the intricate process of tailoring material properties through a multifaceted array of modifications. A detailed breakdown reveals the nuanced techniques employed in this endeavor. The manipulation of thickness stands as a key strategy, involving precise control over material dimensions to influence mechanical, electronic, and optical properties through meticulous adjustments in the fabrication process. Introducing vacancies within the crystal

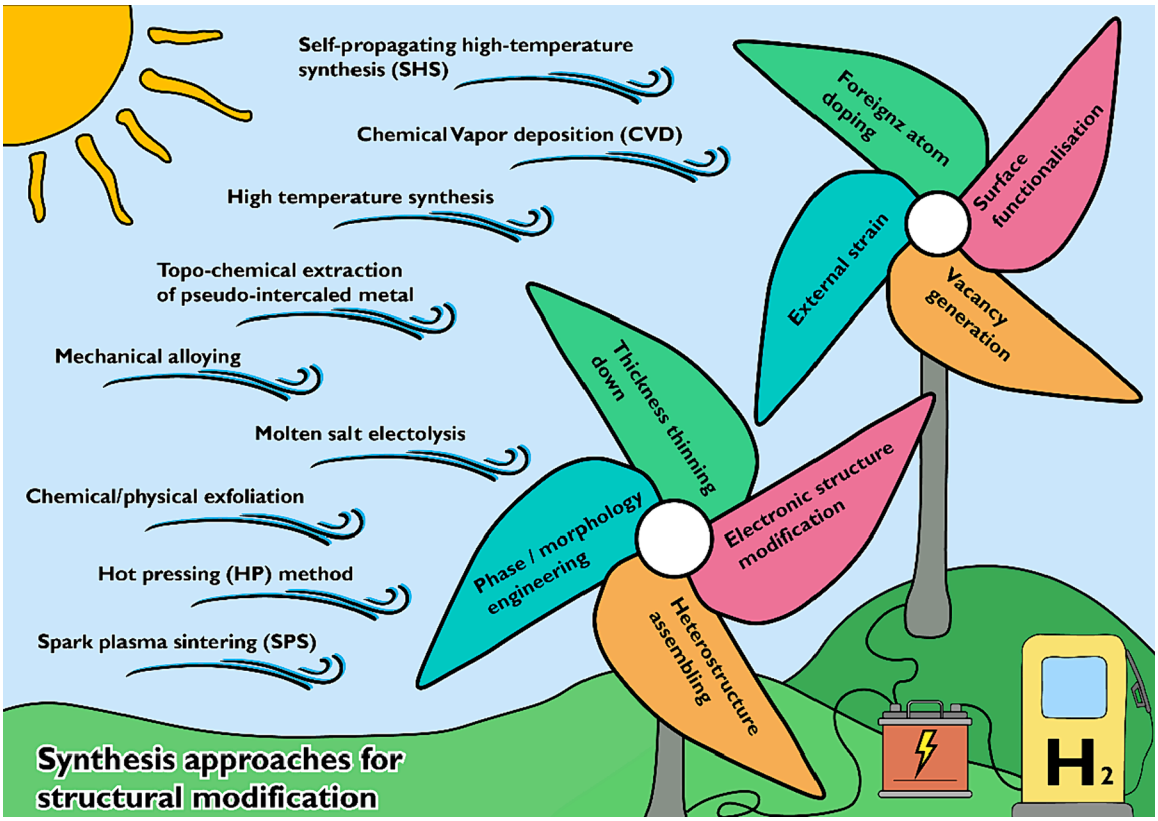

Fig. 12. Scheme on review of modification of electronic structure strategies and different synthesis approaches in tmccs.

lattice structure serves as a deliberate tactic to alter properties such as conductivity, stability, and catalytic activity. Promotion of interactions with foreign species, such as additional atoms or molecules, modifies material behavior, potentially enhancing catalytic activity, improving adsorption capabilities, or altering electronic properties. Surface functionalization, achieved through attaching functional groups or molecules to the material's surface, imparts specific functionalities like increased reactivity, selectivity, or compatibility with other materials. External strain application involves subjecting the material to mechanical stress, deforming its structure, and leading to modifications in electronic band structure, mechanical strength, and other properties. Substitutional doping introduces foreign atoms into the crystal lattice, significantly altering electrical, magnetic, or optical properties. Stacking or assembling heterostructures involves combining different materials or layers to create a composite material with tailored properties, allowing the exploitation of synergistic effects. The complete utilization of these synthesis strategies inspires researchers to finely tune material properties for diverse applications, spanning from electronics, to catalysis, sensing, and energy storage [208,227–230,232]. Fig 12 serves as a visual representation of the elaborate interplay of these synthesis methods in achieving desired material modifications.

5.3.1. *High temperature synthesis*

One of the reasons for the lack of applied research on TMCC might be the difficulty for synthesizing pure phase TM_2S_2C. High temperature synthesis like mechanical alloying, CVD, topo-chemical, combustion self-propagating high-temperature combustion synthesis, mechanical alloying, molten salt electrolysis, chemical/physical exfoliation, and HP method, and SPS can be used to get a pure phase. The process of mechanical alloying is a non-equilibrium technique that has garnered significant interest owing to its remarkable capability to alloy immiscible elements. This method involves milling, where intense deformation leads to a continuous interplay of particle deformation, welding, and fracturing [230]. Combustion synthesis method is preferred because it allows for the production of compounds with uniform composition, fine microstructure, and high purity. However, the reaction conditions must be carefully controlled to avoid side reactions and ensure high yields of the desired product [227]. However, the HP method requires a high temperature (up to 1600 °C) and a long processing time. Very recently, *Majed et al.*, [201] reported the synthesis of a new family of 2D TMCCs by introducing 2D sheets of Nb_2X_2C and Ta_2X_2C via electrochemical intercalation of lithium between the TM_2X_2C layers followed by sonication in water. Synthesis from the metal precursors (like Fe metal, Mn metal, Co metal, Ni metal etc), Sulfur and carbon is challenging because the metal sintering procedure needs an extensively high temperature (>1200 °C). Up to now, the broad group of complex TMCC has only been focused on the aspect of their synthesis condition, structure, and their ability to form intercalation compounds. Recently, the use of TMCC on energy storage (as Li ion battery cathode material) is tested and reported a promising output.

5.3.2. *Topo-chemical extraction of pseudo-intercalated metal*

Topo-chemical extraction of pseudo-intercalated metal involves the removal of metal atoms that are not structurally located in the intercalation sites of a layered material but are instead bonded to the surrounding layers. This process is important for understanding the intercalation chemistry of layered materials, as well as for developing strategies to improve their properties. Intercalation of some

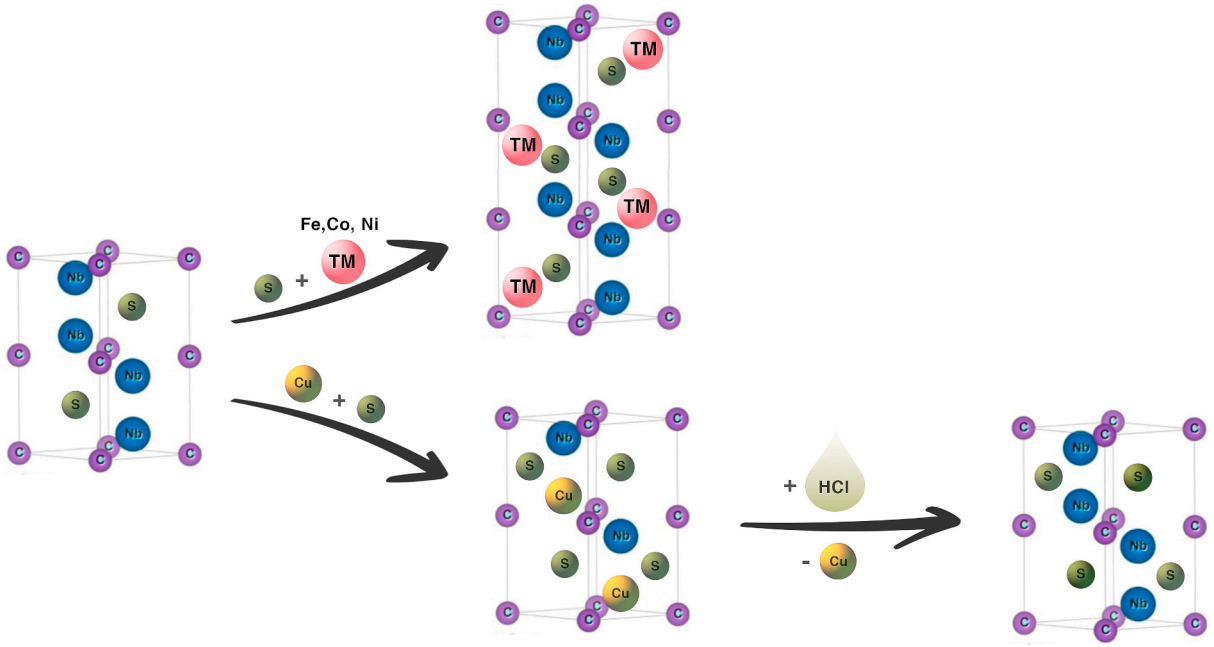

Fig. 13. Topo-chemical reaction scheme of the formation of Tm [Nb_2S_2C] phases and Nb_2S_2C.

unique metals or molecules into the layers of TMCCs, followed by ultra-sonication and magnetic stirring can generate monolayers or few-layers of TMCCs nano-sheets. Furthermore, the pseudo-intercalation method can also be used to synthesize a pure phase of TMCCs after the extraction of the intercalated metal [193,195]. The extraction process typically involves the use of a suitable reagent that can selectively react with the pseudo-intercalated metal, while leaving the intercalated metal intact. The reagent may be a strong acid, a reducing agent, or a chelating agent, depending on the nature of the metal and the surrounding ligands. One example of topo-chemical extraction is the removal of Cu from Cu-intercalated graphite. In this case, the copper atoms are not located in the intercalation sites, but instead form covalent bonds with the surrounding graphene layers. Treatment of the material with hydrochloric acid or nitric acid can selectively dissolve the copper atoms, leaving the graphite layers intact. For instance, H-phase M_2SC synthesized first from the metal (M = Ta, Nb), sulfur and carbon powder precursor. [194] To obtain the 3s-TM_2SC, the H-phase TM_2SC, with pseudo-intercalated metal like V or Cu as depicted in Fig. 13 with a minimum intercalated metal content of 2/3, the process involves sequential steps. Subsequently, the pseudo-intercalated metal component is extracted using iodine in a dehydrated acetonitrile solution with minimal water content, all performed at room temperature, as per the provided equation. [226]

$$Cu_xNb_2S_2C + \frac{x}{2}\mathrm{I} \rightarrow \mathrm{Nb_2S_2C} + x\mathrm{CuI}$$

Topo-chemical extraction of pseudo-intercalated metal can lead to improved properties of the resulting material, such as increased conductivity or improved catalytic activity. It can also provide insights into the intercalation chemistry of layered materials, helping to guide the development of new intercalation strategies. On the other hand, the TMCC sheets synthesized through intercalation/delamination demonstrate larger interlayer spacing and more sites for hybridization with TMCs. The intercalated/delaminated structures result to accommodate more metal ions or small molecules between the individual layers. This would be more favorable for the storage of alkali metal ions and transportation of small molecules in the TMCCs.

Molten salt electrochemical synthesis can also be employed to prepare TMCCs first at low temperatures. However, this method is time-consuming and not convenient for the industrial scale-up production of TMCCs. Combustion synthesis was investigated as one of the best synthesis approaches to obtain high purity of ternary and quaternary carbo-sulfides of the transition metals 2D materials to be tested as solid lubricants in high-temperature environments. The presence of excess carbon reduced the oxygen content of the carbo-sulfide. However, the higher the overall carbon contents, the higher is the amount of carbide impurities in the reaction products. Use of iodine or hexachlorobenzene as a catalyzer minimized the need of excess sulfur in the raw powder mixture, reduced the amount of carbide impurities, and contributed to the homogenization of the reaction products. Similarly, use of HCl, Br_2-CH_3OH, I_2-CH_3OH and $HClO_4$ reduce the presence of excess transition metal or helps to control the composition of metals via metal etching [233]. The choice of synthesis procedure depends on the desired properties and application of the TMCCs. The conditions used in each synthesis procedure, such as temperature, pressure, reaction time, and precursor concentration, play a critical role in determining the properties of the resulting TMCCs.

6. Understanding and Overcoming challenges associated with TMCCs

While pure TMCCs-derived electrode materials have demonstrated noteworthy electrochemical energy storage capabilities, showcasing significant interest in water splitting, as anode materials in Li ion batteries, and Na-ion batteries, the utilization and production of TMCC-based materials with superior properties poses a set of distinct challenges that currently impede their widespread application in diverse catalysis, and batteries. Still, numerous technological challenges need to be addressed to get the adequate benefit of these materials. The main technological challenges and possible tackling approaches are summarized in Fig 14.

The family of TMCCs, Ta_2S_2C, was initially introduced in the early 1970s by Beckmann, Boller, and Nowotny [198]. Two decades later, Boller and Hiebl [195], reported the synthesis of a metastable phase, Nb_2S_2C, sharing a structural resemblance with Ta_2S_2C. This synthesis involved a topochemical reaction initiated with H-Nb_2SC, leading to the formation of $Cu_{0.7}Nb_2S_2C$, followed by the de-intercalation of Cu. Despite these advancements, all reported materials remain in bulk 3D form and have been overshadowed by

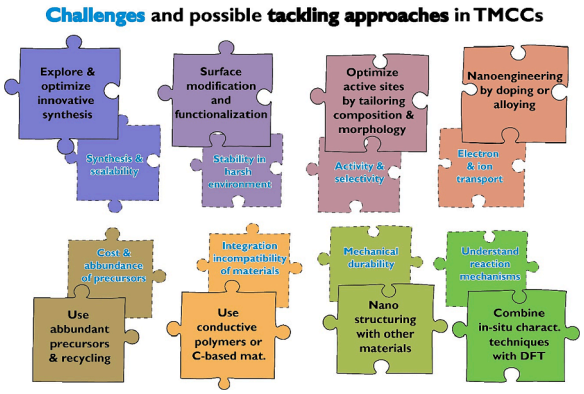

Fig. 14. Key technological challenges and possible tackling approaches in TMCCs.

the prominence of 2D materials. Consequently, the topochemical reaction-based synthesis faces challenges due to its execution at very high temperatures (>1000 ^{O}C) [196,201], along with obstacles related to size control and scalability. However, such high-temperature synthesis methods, including carbothermal reduction or arc melting, are employed to provide the requisite energy for transforming metal oxides or precursors into carbides or nitrides. However, this approach often leads to undesirable particle growth due to increased diffusion rates and agglomeration, resulting in larger crystallite sizes. In applications such as electrocatalysis and energy storage, the particle size of TMCCs plays a pivotal role in determining catalytic activity and electrochemical performance. Larger particle sizes negatively influence catalytic activity by reducing surface area and altering surface properties critical for catalytic reactions. In energy storage applications, the particle size influences ion diffusion kinetics, with larger particles potentially causing slower ion transport and compromising overall device performance. Researchers are actively addressing this challenge by exploring alternative synthesis methods. For instance, low-temperature approaches like sol–gel processes enable controlled nucleation and particle growth with smaller and more uniform sizes, preserving catalytic activity. Exploration of innovative synthesis methods such as sol–gel processes, carbothermal reduction using hydrogen gas as reducing agent [234], or coating with silica based material to prevent particle growth [6], is vital. The synthesis to TMCCs is limited only to Nb, Ti, and Ta. Thus, it is reasonable to assume that other MAX phases (e.g., Ti_2SC, Zr_2SC, and Hf_2SC) can also be used as precursors for new metastable phases, further expanding the compositional space of this new family of 2D TMCCs that can bridge the gap between electrically conductive 2D graphene or MXenes and TMDCs. In tackling the synthesis and scalability challenges of TMCCs, an extensive approach is advocated, supported by specific examples. Exploration of innovative synthesis methods such as sol–gel processes has demonstrated success in achieving controlled and scalable TMCC production. Additionally, researchers are investigating the use of additives and surfactants during high-temperature synthesis to control particle growth. These compounds act as stabilizers, preventing excessive agglomeration and ensuring the formation of smaller, well-dispersed TMCC particles. Notably, this strategy has shown promise in controlling particle size in various metal carbides, as exemplified in a study focused on additives in the synthesis of metal carbides. By addressing the challenge of particle size growth, researchers aim to optimize the performance of TMCCs, making them more effective in catalytic and energy storage applications.

Another issue related to stability of TMCCs in harsh environments underscores the susceptibility of TMCCs to degradation and chemical transformations under extreme conditions, necessitating measures to ensure prolonged stability for sustained electrocatalytic or battery storage performance [196,201]. To address the stability of TMCCs in harsh environments, modification through surface coatings can be an essential approach. For instance, the application of graphene oxide as a protective coating has enhanced the stability of Nb_2Se_2C electrocatalysts under harsh conditions, showcasing the effectiveness of this approach. Similarly, encapsulation strategies have been demonstrated using various polymers, conductive and stable metal oxides (like Ti_4O_7) [6], to shield TMCCs from corrosive environments can provide robust protection for TMCCs nanoparticles.

Achieving optimal electrocatalytic activity and selectivity constitutes an ongoing challenge, demanding a nuanced approach to optimize surface properties, catalytic sites, and electronic structures of TMCCs. Efficient electron and ion transport stand out as critical factors for electrocatalyst and battery material performance, prompting the need for innovative TMCC structures that facilitate rapid diffusion to and from active sites. In practical applications, the integration of TMCCs with other materials is commonplace, demanding efforts to achieve compatibility and synergistic effects for enhanced overall performance. Addressing challenges related to electron and

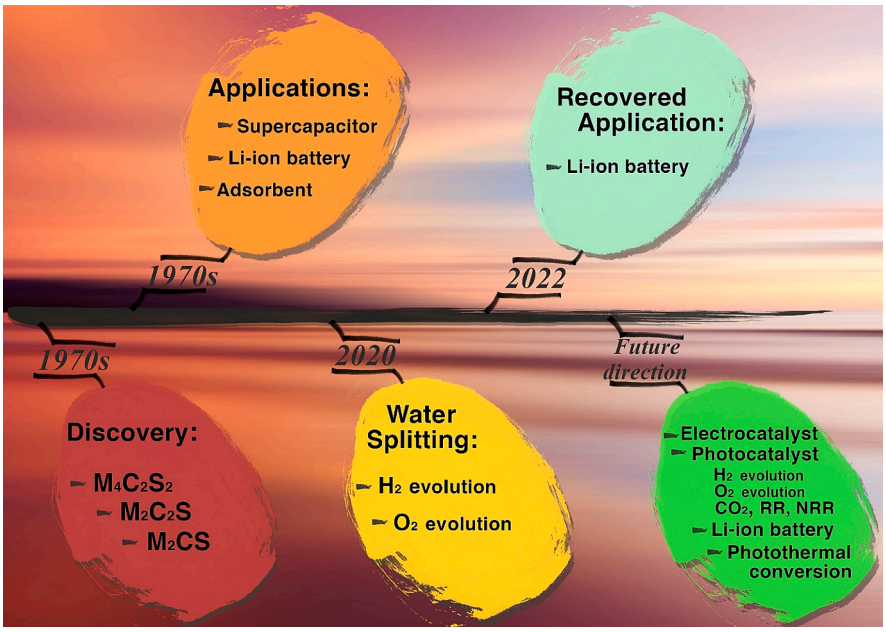

Fig. 15. The chronology of various applications of TMCC; where years are the time when the corresponding TMCC-based composites was first reported.

ion transport involves engineering porous structures within TMCCs, as demonstrated in the synthesis of metal carbide with hierarchical porous structures, facilitating efficient charge transfer in energy storage applications [235,236]. The integration of TMCCs with other materials to enhance overall electrochemical performance has been exemplified in the development of composite materials such as nickel–cobalt nitride/TMCC hybrids, where the optimized interface ensures compatibility and synergistic effects.

Finally, a comprehensive understanding of electrochemical reaction mechanisms at the TMCC surface is indispensable for targeted design and optimization, highlighting the need to bridge knowledge gaps to propel advancements in electrocatalysis and energy storage technologies [195,224]. Addressing these challenges collectively is pivotal for unlocking the full potential of TMCCs in the realm of electrochemical applications [237,238]. In situ characterization techniques are crucial for gaining both thermodynamic and kinetic parameters of the surface reconstruction. Operando characterizations, which can reveal the catalyst evolution at actual working conditions, especially in a water splitting setup with large current density, will provide invaluable information on the mechanism of catalysts degradation.

Theoretical simulations have proven their success in providing valuable insights on the use of TMCCs as catalyst and anode materials for Li ion battery. Finally, the TMCCs' potential applications extend far beyond the ones explored here to other electrochemical energy storage and conversion systems, electronics, sensing, environmental and biological applications.

7. Potential application areas of TMCCs

With the increasing environmental crises and energy demand, renewable energy storage and conversion technologies (battery, and catalysis (water splitting)) have attracted much attention (Fig. 15). The high-efficient catalysts are the key factors of these catalysis technologies in practical applications. However, the practical applications of some catalysts (i.e., precious metals) are always hindered by their high cost and scarcity. Therefore, developing novel efficient catalysts with low costs is urgently necessary. On the one hand, 2D MXenes with high conductivity, low costs, rich active sites, and abundant surface termination groups are widely utilized as catalysts and catalyst hosts for electro catalysis, photocatalysis and as anode material for Li ion battery. In connection to the development of active and stable catalysts, various synthesis methods have been developed to expose abundant active sites on the surface. Given the exposed active surfaces, confinement guarantees long-term application of the catalysts, in addition to enhancing their intrinsic activity. The following subsections highlight the progress so far in applying space confined catalysis for different kinds of reactions. On the other hand, the chemistry behind transition metal carbides brings here a great opportunity. These compounds are often referred to as

Table 2
Summary of TMDs, MXenes and TMCCs in water oxidation and anode material in Li ion battery.

Class of materials	Catalysts	Application					
		OER			Battery		
		overpotential@10 ($mAcm^{-1}$)	Stability/ hr	Ref.	Material	Specific capacities ($mAhg^{-1}$)	Ref.
TMDs	Fe-MoS_2	290	25	[66]	2D MoS_2 nanosheets	1009.2	[73]
	MoS_2/CoS_2	290	26	[67]	2D SnS_2 nanoplates	323	[74]
	NiSe	290	12	[68]	Mo doped SnS_2	1950.8	[75]
	$MoWS_2/Ni_3S_2$	390	50	[69]	SnS_2/ MoS_2	1294	[76]
	Co/MoS_2	260	3000 cycles	[70]	MoO_3/SnS_2	504	[77]
	$CoTe_2$@Ni	310	27	[71]	WS_2 nanosheets	118	[78]
	$NiTe_2$/Ni $(OH)_2$	267	6	[72]	VS_2/graphene	180.1	[79]
MXenes	FeOOH NSs@$Ti_3C_2T_x$	400	30	[239]	Nb_2CO_2	292	[240]
	Co@V_2CT_x	242	10	[241]	Nb_2CT_x	448	[242]
	Co@Nb_2CT_x	310	10	[241]	S-decorated $Ti_3C_2T_x$	167.8	[243]
	Co@Ti_3CT_x	388	10	[241]	$Hf_3C_2T_z$	145	[244]
	$MoSe_2/Ti_3C_2T_x$	340	50	[245]	$Ti_3C_2T_x$/CNT	1250	[246]
	CoP/$Ti_3C_2T_x$	230	24	[247]	Nb_2O_5@$Nb_4C_3T_x$	208	[248]
	MOOH @$V_4C_3T_x$	275.2	70	[249]	V_2CTx	185	[250]
TMDs- Mxenes heterostructure	MoS_2/MXene	410	50	[245]	$MoS_2/Mo_2TiC_2T_x$	554	[165]
	Ni–$MoSe_2/Ti_2NT_x$	270	18	[251]			
	2D CoS-Mo_2TiC_2	310	25	[178]			
	$CoSe_2$-2D $Ti_3C_2T_x$	270	12	[252]			
TMCCs	Nb_2Se_2C	321	24	[196]	*m*-Nb_2S_2C	230	[201]
					m-Ta_2S_2C	100	[201]
					Nb_2CSe_2	390	[197]
					MoS_2/Ti_2CS_2	323	[224]
					MoS_2/V_2CS_2	317	
					V_2CS_2	301	

"interstitial alloys," which are prepared by integrating carbon atoms into the interstitial sites of their parent metals. This framework gives rise to the catalytic properties of metal carbides resembling that of noble metals. Combining these two families as one integrated 2D layered structure gives TMCC high conductivity, unique mechanical property, variability of transition metals and termination groups. This combination finds enormous potential applications in a wide range of fields. The following subgroups highlight the advancements so far in applying TMCC catalysis for different types of applications like conversion and storage (for instance as cathode materials in Li-S and Na-S batteries). It can also be used in electro-catalysis for a variety of chemical reactions, water splitting as oxygen evolution catalyst. Lastly, TMCCs exhibit also superconductivity, making them promising for use in superconducting electronics and other applications. The use of TMDs, Mxenes and TMCCs in water oxidation and anode material for Li ion battery are summarized in Table 2 above.

7.1. Rechargeable batteries

This section briefly reviews the potential of TMCCs as anode material for battery. Efficient and eco-friendly energy storage technologies are essential to accommodate the rise of new energy sources. Rechargeable metal ion batteries, including Li^+, Na^+, K^+, and Mg^{2+} variants, are pivotal in portable electronics and electric vehicles [205]. The performance of these batteries' hinges on electrode materials, with layered materials being favored for their reversible ion intercalation capability [196,201,205]. Notably, 2D materials exhibit promise as electrode contenders due to their high surface-to-volume ratio, swift ion diffusion, rapid charge transport, and enhanced reaction kinetics. However, anode materials derived from layered substances encounter challenges related to capacity and safety. Addressing these concerns involves strategies like metal alloying and the creation of hybrid heterostructures to enhance

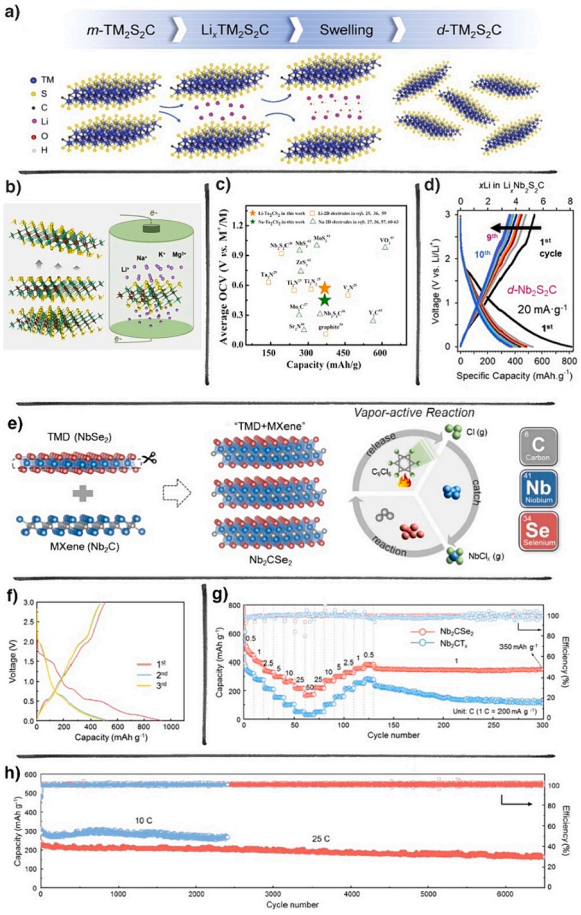

Fig. 16. Synthesis and performance of nb_2S_2C. (a) m-Nb_2S_2C and m-Ta_2S_2C phases synthesis. Reproduced with permission from Ref [201] Copyright 2022, Wiley. (b) TMCCs for various battery applications. Reproduced with permission from Ref [205] Copyright 2019, American Chemical Society. (c) Capacities of Ta_2CS_2 electrode in Li and Na battery Reproduced with permission from Ref [256] Copyright 2020, American Chemical Society (d) Rate capability of d-Nb_2S_2C in a Li-ion battery at Voltage profile of the first 10 cycles at 20 $mA{\cdot}g^{-1}$. Reproduced with permission from Ref [201] Copyright 2022, Wiley. (e) One-step preparation process of Nb_2CSe_2 through a "vapor-active reaction". (f) GCD curves of Nb_2CSe_2 in the first three cycles. (g) Rate performance of Nb_2CSe_2 and Nb_2CT_x. (h) Long-term cycling stability of Nb_2CSe_2. Figures e-g are reproduced with permission from Ref [197], Copyright 2023, Elsevier.

conductivity, battery cycle stability, and overcome capacity limitations. Another avenue entails the exfoliation of novel 2D materials from bulk layered counterparts. Despite these advancements, obstacles remain, such as maintaining interface stability in heterostructure 2D materials and comprehending and manipulating solid/solid interfaces [201]. An innovative category of two-dimensional materials has emerged for energy storage, known as TMCCs [253]. These materials, exemplified by compounds like Nb/Ta/Ti_2S_2C, exhibit favorable traits including strong electrical conductivity, remarkable ion mobility, and satisfactory capacity [224]. The synthesis process of these materials is illustrated in Fig. 16a [205]. The broader vdW gap of TMCC compounds compared to TMDs/TMCs makes their unit cell parameter remaining unaffected after Li intercalation [254]. Moreover, their high electronic conductivity, excellent ion mobility, and ability to create sufficient paths for lithium ions make them ideal for Na, Mg, K, and Li-ion batteries (Fig. 16b, c). The TMCCs can also be used in the development of Li-S and Na-S batteries as active materials for the cathode. However, different factors like delamination, intercalation, and different phase design affect electrochemical properties of these 2D new family materials. To investigate the influence of delamination and phase design on the electrochemical properties of TMCCs, *Majed et al*, examined both *m*-Nb_2S_2C and *d*-Nb_2S_2C as potential electrode materials for LIBs. In Fig. 16d, they employed a rate handling capability test to compare the lithium storage capacity of *d*-Nb_2S_2C and *m*-Nb_2S_2C. Across all tested rates, the average specific capacity of *d*-Nb_2S_2C was approximately three times that of m-Nb_2S_2C. The increased capacity of *d*-Nb_2S_2C can be attributed to enhanced Li accessibility due to delamination of Nb_2S_2C, following the pattern seen in other 2D materials [255], as well as a lower presence of inactive species [256]. X. Yuan *et al.* [224] have also determined the theoretical capacity of the TMCCs family. Theoretical capacities of M_2CS_2 (M = Ti, V) for Na ion battery (NIBs, approximately 400 mAh/g) or Li ion battery (LIBs, approximately 320 mAh/g) are calculated. This illustrates the suitability of M_2CS_2 as anode materials for NIBs/LIBs. The higher capacities indicate that M_2CS_2 present more promising prospects as candidates for NIBs compared to LIBs. Recently, X. Pang and coworkers successfully synthesized the novel Se-terminated niobium carbide MXene (Nb_2CSe_2) with a structure resembling "TMD + MXene." This achievement was realized through a one-step "vapor-active" method (Fig. 16e), eliminating the need for acid etching, and significantly improving the yield to approximately 99 wt%. Nb_2CSe_2 displays remarkable conductivity (7.14×10^4 S m^{-1}), surpassing the conventional MXene Nb_2CT_x (T = O/OH/F) by over 2000 times. At high rates, Nb_2CSe_2 exhibits exceptional performance with a high-rate capacity of 270 mAh/g at 10 C and 170 mAh/g at 50 C, outperforming many reported MXenes-based materials, which typically achieve less than 200 mAh/g at 10 C. Furthermore, Nb_2CSe_2 demonstrates an extended cycling lifespan of over 6,500 cycles at 25 C without noticeable decay. This advancement holds promise for simplifying MXene preparation processes and enhancing the performance of energy storage materials. [197] Table 2 summarize the recent progress in the electrochemical properties of TMCCs as water oxidation catalyst and Li battery anode materials, respectively.

7.2. Water splitting reactions

To date, various TMDs [212] (e.g., SnS_2, MoS_2, Ni_3S_2, and $MoSe_2$) and their composites are utilized in water splitting, metal air battery electrocatalysts (Fig. 17a), to speedup OER, HER, HOR and ORR. Their excellent performance in energy storage and conversion results from the abundant active sites. Nevertheless, the TMD materials suffer from inherent poor conductivity, low chemical stability or insufficient electronic transport ability, and the tendency of aggregation during the electro catalysis reaction. Combining TMDs with 2D conductive MXenes can effectively improve the electronic conductivity and electro catalytic performance. TMDs and MXenes (Fig. 17b) have attracted great attention in electrochemistry due to their tunable electronic structures. However, in this combination, understanding and designing the solid/solid interface is challenging. Inspired by these findings, *Pang et al.*, [196] report the synthesis

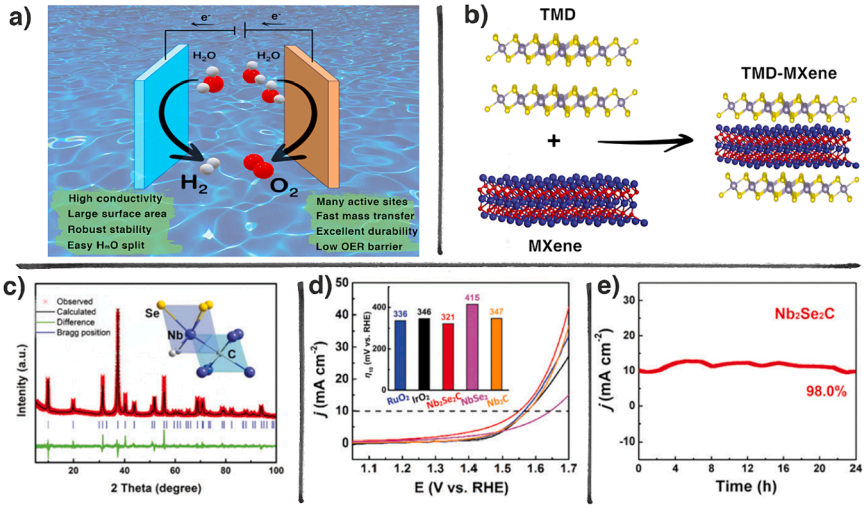

Fig. 17. (a) Schematic illustration of the TMCC for over-all water splitting. (b) The crystal structure of the Nb_2Se_2C. (c) Rietveld refinement of Nb_2Se_2C. (d) OER polarization curves of Nb_2Se_2C, $NbSe_2$, Nb_2C, RuO_2, and IrO_2. (e) Stability test by chronoamperometry for Nb_2Se_2C. (c-e) Reproduced with permission from Ref [196], Copyright 2020, Royal Society of Chemistry.

of a new member of the family of 2D TMCC i.e Nb_2Se_2C that has never been investigated as a catalyst so far is synthesized as the 'TMD–MXene' like compound by replacing the M (e.g., Nb) motifs in a TMD (MX_2: e.g., $NbSe_2$) with the M-X (e.g., Nb–C) motifs in a MXene ($M_{n+1}X_n$: n = 1, e.g., Nb_2C). This material is formed from the combination of TMD and MXenes that associates good conductivity, enriched active sites, low cost, and simple process. The M-C layers and more marginalized Se layers are believed to exhibit good OER performance. The efficiency and effectiveness of optimal electro catalysts are defined based on the different parameters of OER and ORR such as, onset potential, electrochemical surface area, current density, Tafel slope, turnover frequency, half-wave potential, and potential gap. Pang *et al.* reported the synthesis of powder Nb_2Se_2C at 1473 K temperature and studied the OER performance in a 1.0 M KOH solution. As shown in Fig. 17d, this new design of Nb_2Se_2C OER electrocatalyst performs well with a low overpotential of 321 mV at 10 $mAcm^{-2}$, which is lower than its counter parts like Nb_2C (347 mV), $NbSe_2$ (415 mV), IrO_2 (346 mV), RuO_2 (336 mV) [196], and other reported TMDs [257–260], and MXenes electro catalysts in alkaline electrolytes. The enhanced result arises from the interplay among carbon atoms, the existence of more active Se layers, and the additional valence electrons present between Nb (Ta) and Se in the Nb_2Se_2C particles. Moreover, the antibonding orbit exhibits a greater number of occupied electrons, leading to an elongated Nb–Se (Ta–Se) bond and more energetic Se atoms in Nb_2Se_2C and Ta_2Se_2C. This suggests that the peripheral Se atoms in Nb_2Se_2C and Ta_2Se_2C remain chemically active, exhibiting a notable increase in size compared to $NbSe_2$. The Se–Nb–Se angle in Nb_2Se_2C is narrower (77.93°) than in $NbSe_2$ (86.57°), and the Se–Ta–Se angle is approximately 78.31° (refer to Table 2). The larger valence electron cloud of Se atoms and the heightened polarization of the $NbSe_3C_3$ octahedron in Nb_2Se_2C contribute to an increased vdW force between layers. Consequently, the vdW gap is smaller in Nb_2Se_2C (3.041 Å) compared to $NbSe_2$ (3.145 Å). Due to this, the M_2X_2C family of materials have promising and outstanding performance towards water oxidation [196,200]. The metallic Nb–C layers offers excellent conductivity and enriched active sites due to the more marginalized Se layers that make it easier to react with the hydroxyl groups and release O_2. In electro/photo catalysis, TMCCs are good candidates due to their outstanding physical and chemical properties, especially having electrical conductivity, a large surface area, and good chemical and thermal stability (Fig. 17e).

8. Future outlook and conclusion

Recent advances in 2D materials research have led to the discovery of new materials with unique physical and chemical properties, including TMCCs. These materials offer massive structural and chemical diversity, combining the characteristics of TMC MXenes and TMDs at the atomic level. However, the electrochemical application of 2D materials is limited by low chemical stability and insufficient electronic transport ability. Therefore, the development of effective and durable TMCC catalysts is crucial. In this review, we

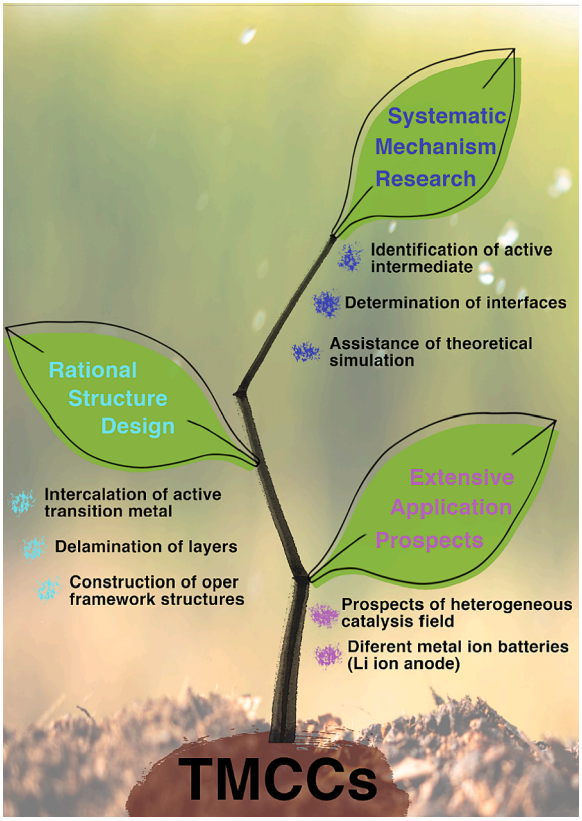

Fig. 18. Perspective for future research transition metal carbo chalcogenides in catalysis.

provided a summary on systematic mechanism research, rational structure design and extensive application prospects (Fig. 18) of TMCC materials. Furthermore, different synthesis methods used to fabricate TMCCs, including wet chemistry strategies, photochemical reduction, metal ion intercalation, atomic layer deposition, confinement strategy, and delamination are also reviewed. We also highlight recent progress in tuning the active site microenvironments of TMCCs through intercalation and delamination, which is pivotal in illustrating the correlation between the structure configuration of TMCCs and their catalytic activity. Finally, we review the typical applications of TMCCs in electrocatalysis, batteries (Li-ion, Na-ion), and other applications such as CO_2 reduction and nitrogen reduction, with abundant examples.

Ongoing research is focused on exploring the potential applications of TMCCs in areas like energy storage, electronic devices, and catalysis. Scientists are trying to understand the complex physics behind these materials, especially the interaction between their electronic and structural properties. Challenges in synthesizing 2D TMCC flakes and modifying their electronic properties persist. TMCCs show promise as catalysts for processes like water splitting, but there are hurdles to overcome, including the need for more efficient synthesis methods and the exploration of alternative metals and intercalation techniques. Understanding the evolution of TMCCs is crucial for designing practical applications, and there is a need for cost-effective, selective, and stable electrocatalysts for high current density water splitting. In summary, TMCCs offer exciting possibilities across various fields, but further research and development are necessary to unlock their full potential. Some of the potential areas where TMCCs hold a highly promising application are:

Energy Storage: TMCCs have shown promising potential as electrode materials in energy storage devices such as batteries and supercapacitors. Their high specific capacitance, excellent cycling stability, and fast charge–discharge rates make them attractive candidates for next-generation energy storage systems. Future research will focus on optimizing TMCC compositions and structures to enhance their electrochemical performance and further improve energy storage capabilities.

Catalysis: TMCCs exhibit remarkable photo/electrocatalytic activity, which can be attributed to the synergistic effects between TM, C, and S/Se. The TMCCs exhibit outstanding tensile strength owing to their remarkable anisotropic high elasticity. Additionally, a comprehensive investigation was conducted on various optical properties, including the dielectric function, absorption, reflectance, and optical conductivity. In the ultraviolet spectrum, X_2Se_2C (X = Ta, Nb) emerges as an efficient absorber with a notable high refractive index. Ongoing efforts will involve exploring new TMCC compositions, surface modifications, and heteroatom doping to enhance catalytic efficiency and selectivity for sustainable energy conversion processes. Additionally, TMCCs can also be best candidate in the synthesis of valuable chemicals like oxidation, reduction, bond activation and functionalization of various organic and inorganic substrates, including HMF, glycerol, benzyl alcohol, O_2, N_2, etc. It can also be applied in photo/electrochemical N_2 reduction for NH_3 synthesis, ORR to H_2O_2, H_2O_2 synthesis and C–H and C–C bond activation and functionalization. The development of various types of TMCCs based on 2D materials can also offer substantial applications in electro/photo catalysis of CO_2 reduction/syngas conversion in to CH_4, CH_3OH, C_2H_5OH and CO oxidation. [261] Thus, it is highly important to develop and explore selective catalyst toward the desired product. Based on the types of reduction yields, metal catalysts are categorized into different major groups denoted as (i) CO selective (Zn, Ga, Pd, Ag, Au), (ii) format selective (Sn, In, Hg, Pb), (iii) HER (Ti, Fe, Ni, Pt) favorable electrocatalyst and (iv)

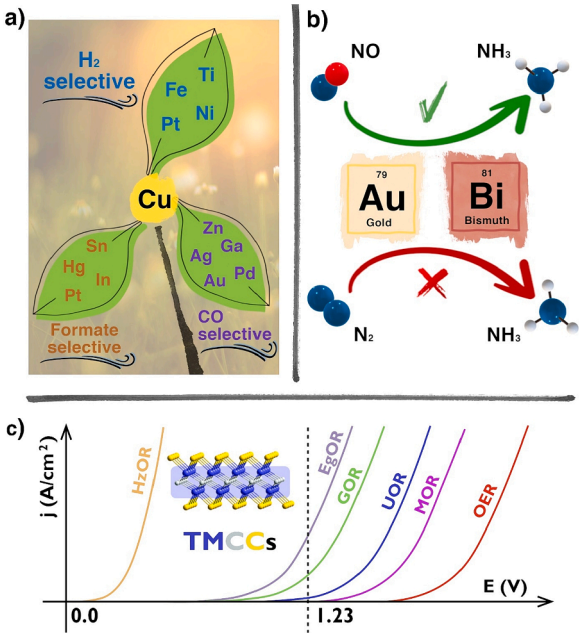

Fig. 19. Schematic illustration for transition metals favorable for (a) different CO_2 products selective and (b) NO and NRR selective electro catalysts. (c). different application areas of TMCCs as electrocatalyst (c). Possible application of TMCCs in different areas of catalysis (HzOR, EgOR, GOR, UOR, MOR and OER).

hydrocarbon (CH_4 and C_2H_4) catalysts, in which hydrocarbons are significantly and uniquely formed together with other products on Cu electrocatalyst. However, those new families of 2D TMCC materials have not been tried in CO_2 reduction/syngas conversion so far.

Hence, we propose the utilization of these innovative catalyst families (depicted in Fig. 19a) to propel advancements in the field by selectively introducing metals (such as Cu, Sn, In, Ag, etc.) into the layers of TM_2S_2C, resulting in product selective $TM_xNb_2S_2C$, $TM_xTa_2S_2C$ for CO, CH_4, HCOOH, CH_3OH, and C_2H_5OH reactions. Due to the enhanced activity, and stability, TMCC materials has been employed in energy conversion and storage devices, [196] and also acknowledged for accelerating reactions like OER hydrazine oxidation reaction (H_zOR), ethylene glycol oxidation reaction (E_gOR), HER, ORR, UOR, MOR and NRR (Fig. 19b,c). TMCSs can also be efficient catalysts in electroreduction of NO_2^-, NO_3^-, NO, and NO_2^- to possible by-products, such as NH_3, N_2, NO, NH_2OH and H_2. Further to bring an effect on the activity and conductivity of TMCCs modification of the surface functionalization, exfoliation/delamination yield, and defect concentration are important factors. Furthermore, the high electrical conductivity, and large specific surface area properties make TMCCs the best competent electrodes in super-capacitors.

Electronics and Optoelectronics: TMCCs possess intriguing electronic properties, making them promising candidates for electronic and optoelectronic devices. Their tunable bandgaps, high carrier mobility, and strong light-matter interactions enable applications in areas such as transistors, photodetectors, light-emitting diodes (LEDs), and solar cells. Continued research will focus on developing scalable synthesis methods, improving material quality, and exploring novel device architectures to harness the full potential of TMCCs in these fields.

Sensing and Detection: TMCCs offer excellent sensing capabilities due to their high surface-to-volume ratios and unique chemical reactivity. They can be utilized for gas sensing, biosensing, and environmental monitoring applications. Future research will explore the integration of TMCCs with nanomaterials, such as graphene and metal nanoparticles, to enhance sensing performance and enable selective and sensitive detection of various analytes.

Emerging Applications: As research progresses, new applications for TMCCs are likely to emerge. Their multifunctional nature and the ability to tailor their properties through compositional and structural modifications make them attractive for a wide range of fields, including flexible electronics, photonics, thermoelectrics, and water splitting for hydrogen generation. Future investigations will uncover the full extent of TMCCs' potential in these and other exciting areas.

To fully realize the future potential of TMCCs, interdisciplinary collaborations between materials scientists, chemists, physicists, and engineers will be essential. Additionally, advances in computational modeling and simulation techniques will aid in understanding the underlying properties and guiding the design of novel TMCC materials. Despite the progress made in recent years, continued research, and technological advancements in TMCC synthesis, characterization, and device integration will unlock their full potential, leading to significant advancements in multiple scientific and technological domains.

CRediT authorship contribution statement

Kassa Belay Ibrahim: Conceptualization, Data curation, Formal analysis, Investigation, Writing – original draft. **Tofik Ahmed Shifa:** Data curation, Formal analysis, Methodology, Writing – original draft. **Sandro Zorzi:** Formal analysis, Investigation, Methodology, Validation. **Marshet Getaye Sendeku:** Data curation, Formal analysis, Investigation, Writing – original draft. **Elisa Moretti:** Conceptualization, Funding acquisition, Supervision, Writing – review & editing. **Alberto Vomiero:** Conceptualization, Funding acquisition, Supervision, Writing – review & editing.

Declaration of competing interest

The authors declare that they have no known competing financial interests or personal relationships that could have appeared to influence the work reported in this paper.

Data availability

No data was used for the research described in the article.

References

[1] Sendeku MG, Shifa TA, Dajan FT, Ibrahim KB, Wu B, Yang Y, et al. Advanced Materials, n/a, 2308101.
[2] Ibrahim KB, Tsai M-C, Chala SA, Berihun MK, Kahsay AW, Berhe TA, et al. J Chin Chem Soc 2019;66:829–65.
[3] Birhanu MK, Tsai M-C, Kahsay AW, Chen C-T, Zeleke TS, Ibrahim KB, et al. Adv Mater Interfaces 2018;5:1800919.
[4] Chala SA, Tsai M-C, Su W-N, Ibrahim KB, Thirumalraj B, Chan T-S, et al. ACS Nano 2020;14:1770–82.
[5] Chala SA, Tsai M-C, Su W-N, Ibrahim KB, Duma AD, Yeh M-H, et al. ACS Catal 2019;9:117–29.
[6] Ibrahim KB, Su W-N, Tsai M-C, Chala SA, Kahsay AW, Yeh M-H, et al. Nano Energy 2018;47:309–15.
[7] Ibrahim KB, Su WN, Tsai MC, Kahsay AW, Chala SA, Birhanu MK, et al. Mater Today Chem 2022;24:100824.
[8] Xu K, Yin L, Huang Y, Shifa TA, Chu J, Wang F, et al. Nanoscale 2016;8:16802–18.
[9] Wang F, Shifa TA, Zhan X, Huang Y, Liu K, Cheng Z, et al. Nanoscale 2015;7:19764–88.
[10] Yu P, Wang F, Shifa TA, Zhan X, Lou X, Xia F, et al. Nano Energy 2019;58:244–76.
[11] Chia X, Eng AYS, Ambrosi A, Tan SM, Pumera M. Chem Rev 2015;115:11941–66.
[12] Wilson JA, Yoffe A. Adv Phys 1969;18:193–335.
[13] Keum DH, Cho S, Kim JH, Choe D-H, Sung H-J, Kan M, et al. Nat Phys 2015;11:482–6.
[14] Barrera D, Wang Q, Lee Y-J, Cheng L, Kim MJ, Kim J, et al. J Mater Chem C 2017;5:2859–64.
[15] Kalanyan B, Kimes WA, Beams R, Stranick SJ, Garratt E, Kalish I, et al. Chem Mater 2017;29:6279–88.

[16] Zeng Z, Sun X, Zhang D, Zheng W, Fan X, He M, et al. Adv Funct Mater 2019;29:1806874.
[17] Horiba K, Ono K, Oh J, Kihara T, Nakazono S, Oshima M, et al. Phys Rev B 2002;66:073106.
[18] Aiura Y, Bando H, Kitagawa R, Maruyama S, Nishihara Y, Horiba K, et al. Phys Rev B 2003;68:073408.
[19] Bovet M, Popović D, Clerc F, Koitzsch C, Probst U, Bucher E, et al. Phys Rev B 2004;69:125117.
[20] Suzuki M-T, Harima H. Phys B Condens Matter 2005;359–361:1180–2.
[21] Wu Y, Xing H, Lian C-S, Lian H, He J, Duan W, et al. Phys Rev Mater 2019;3:104003.
[22] Martinez H, Auriel C, Gonbeau D, Loudet M, Pfister-Guillouzo G. Appl Surf Sci 1996;93:231–5.
[23] Fang CM, de Groot RA, Haas C. Phys Rev B 1997;56:4455–63.
[24] Slough CG, Giambattista B, Johnson A, McNairy WW, Wang C, Coleman RV. Phys Rev B 1988;37:6571–4.
[25] Kidd T, Miller T, Chou M, Chiang T-C. Phys Rev Lett 2002;88:226402.
[26] Cercellier H, Monney C, Clerc F, Battaglia C, Despont L, Garnier MG, et al. Phys Rev Lett 2007;99:146403.
[27] Eda G, Yamaguchi H, Voiry D, Fujita T, Chen M, Chhowalla M. Nano Lett 2011;11:5111–6.
[28] Guo Y, Sun D, Ouyang B, Raja A, Song J, Heinz TF, et al. Nano Lett 2015;15:5081–8.
[29] Xiong F, Wang H, Liu X, Sun J, Brongersma M, Pop E, et al. Nano Lett 2015;15:6777–84.
[30] Jung Y, Zhou Y, Cha JJ. Inorg Chem Front 2016;3:452–63.
[31] Xia J, Wang J, Chao D, Chen Z, Liu Z, Kuo J-L, et al. Nanoscale 2017;9:7533–40.
[32] He Q, Lin Z, Ding M, Yin A, Halim U, Wang C, et al. Nano Lett 2019;19:6819–26.
[33] Zhan G, Quan F, Yao Y, Zhao S, Liu X, Gu H, et al. Appl Catal B 2023;323:122186.
[34] Li P-Z, Chen N, Al-Hamry A, Sheremet E, Lu R, Yang Y, et al. Chem Eng J 2023;457:141289.
[35] Wang F, Li Y, Shifa TA, Liu K, Wang F, Wang Z, et al. Angew Chem Int Ed 2016;55:6919–24.
[36] Wang F, Wang Z, Shifa TA, Wen Y, Wang F, Zhan X, et al. Adv Funct Mater 2017;27:1603254.
[37] Kirubasankar B, Won YS, Adofo LA, Choi SH, Kim SM, Kim KK. Chem Sci 2022;13:7707–38.
[38] Wang X, Wu J, Zhang Y, Sun Y, Ma K, Xie Y, et al. Adv Mater 2023;35:2206576.
[39] Ozden B, Zhang T, Liu M, Fest A, Pearson DA, Khan E, et al. ACS Nano 2023;17:25101–17.
[40] Price CC, Frey NC, Jariwala D, Shenoy VB. ACS Nano 2019;13:8303–11.
[41] Parvin S, Hazra V, Francis AG, Pati SK, Bhattacharyya S. Inorg Chem 2021;60:6911–21.
[42] Stark MS, Kuntz KL, Martens SJ, Warren SC. Adv Mater 2019;31:1808213.
[43] Chen X, McDonald AR. Adv Mater 2016;28:5738–46.
[44] Presolski S, Pumera M. Mater Today 2016;19:140–5.
[45] Voiry D, Goswami A, Kappera R Silva CdCCe, Kaplan D, Fujita T, Chen M et al. Nat Chem 2015;7:45–49.
[46] Lu N, Guo H, Li L, Dai J, Wang L, Mei W-N, et al. Nanoscale 2014;6:2879–86.
[47] Roldán R, Castellanos-Gomez A, Cappelluti E, Guinea F. J Phys Condens Matter 2015;27:313201.
[48] Loh L, Zhang Z, Bosman M, Eda G. Nano Res 2021;14:1668–81.
[49] Gao H, Suh J, Cao MC, Joe AY, Mujid F, Lee K-H, et al. Nano Lett 2020;20:4095–101.
[50] Wang S, Cui X, Jian Ce, Cheng H, Niu M, Yu J, et al. Adv Mater 2021;33:2005735.
[51] Han SS, Ko T-J, Yoo C, Shawkat MS, Li H, Kim BK, et al. Nano Lett 2020;20:3925–34.
[52] Jaramillo TF, Jørgensen KP, Bonde J, Nielsen JH, Horch S, Chorkendorff I, Science, 2007;317:100-102.
[53] Chowdhury T, Sadler EC, Kempa TJ. Chem Rev 2020;120:12563–91.
[54] Shi J, Wu D, Zheng X, Xie D, Song F, Zhang X, et al. physica status solidi (b) 2018;255:1800254.
[55] Wu N, Yang Z, Zhou W, Zou H, Xiong X, Chen Y, et al. J Appl Phys 2015;118:084306.
[56] Yuan S, Pang S-Y, Hao J. Appl Phys Rev 2020;7:021304.
[57] Kobayashi K, Yamauchi J. Phys Rev B 1995;51:17085.
[58] Radisavljevic B, Radenovic A, Brivio J, Giacometti V, Kis A. Nat Nanotechnol 2011;6:147–50.
[59] Terrones H, Terrones M. 2D Materials 2014;1:011003.
[60] Hinsche NF, Thygesen KS. 2D Materials 2017;5:015009.
[61] Lopez-Sanchez O, Lembke D, Kayci M, Radenovic A, Kis A. Nat Nanotechnol 2013;8:497–501.
[62] Britnell L, Ribeiro RM, Eckmann A, Jalil R, Belle BD, Mishchenko A, et al. Science 2013;340:1311–4.
[63] Lee HS, Min S-W, Chang Y-G, Park MK, Nam T, Kim H, et al. Nano Lett 2012;12:3695–700.
[64] Tsai D-S, Liu K-K, Lien D-H, Tsai M-L, Kang C-F, Lin C-A, et al. ACS Nano 2013;7:3905–11.
[65] Sundaram R, Engel M, Lombardo A, Krupke R, Ferrari A, Avouris P, et al. Nano Lett 2013;13:1416–21.
[66] Xue J-Y, Li F-L, Zhao Z-Y, Li C, Ni C-Y, Gu H-W, et al. Inorg Chem 2019;58:11202–9.
[67] Zhou G, Wu X, Zhao M, Pang H, Xu L, Yang J, et al. ChemSusChem 2021;14:699–708.
[68] Chen D, Chen Y, Zhang W, Cao R. New J Chem 2021;45:351–7.
[69] Zheng M, Du J, Hou B, Xu C-L. ACS Appl Mater Interfaces 2017;9:26066–76.
[70] Xiong Q, Wang Y, Liu P-F, Zheng L-R, Wang G, Yang H-G, et al. Adv Mater 2018;30:1801450.
[71] Yin Y, Xu J, Guo W, Wang Z, Du X, Chen C, et al. Electrochim Acta 2019;307:451–8.
[72] Xu B, Yang X, Liu X, Song W, Sun Y, Liu Q, et al. J Power Sources 2020;449:227585.
[73] Zhang S, Chowdari BVR, Wen Z, Jin J, Yang J. ACS Nano 2015;9:12464–72.
[74] Seo Jw, Jang Jt, Park Sw, Kim C, Park B,Cheon J. Adv Mater 2008;**20**:4269-4273.
[75] Chen Q, Lu F, Xia Y, Wang H, Kuang X. J Mater Chem A 2017;5:4075–83.
[76] Voiry D, Salehi M, Silva R, Fujita T, Chen M, Asefa T, et al. Nano Lett 2013;13:6222–7.
[77] Hu C, Shu H, Shen Z, Zhao T, Liang P, Chen X. PCCP 2018;20:17171–9.
[78] Larcher D, Tarascon JM. Nat Chem 2015;7:19–29.
[79] Zeng X, Ding Z, Ma C, Wu L, Liu J, Chen L, et al. ACS Appl Mater Interfaces 2016;8:18841–8.
[80] Sachin S, Rani S, Kumari P, Kar S, Ray SJ. Appl Phys A 2022;129:46.
[81] Xu J, Shim J, Park J-H, Lee S. Adv Funct Mater 2016;26:5328–34.
[82] Chhowalla M, Shin HS, Eda G, Li L-J, Loh KP, Zhang H. Nat Chem 2013;5:263–75.
[83] Lin L, Sherrell P, Liu Y, Lei W, Zhang S, Zhang H, et al. Adv Energy Mater 2020;10:1903870.
[84] Voiry D, Mohite A, Chhowalla M. Chem Soc Rev 2015;44:2702–12.
[85] Hoang Huy VP, Ahn YN, Hur J. Nanomaterials 2021;11:1517.
[86] Gogotsi Y, Anasori B. ACS Nano 2019;13:8491–4.
[87] Verma C, Zehra S, Aslam R, Aslam J, Quraishi MA, Mobin M. Adv Mater Interfaces 2022;9:2200579.
[88] Nat Nanotechnol 2022;17:1025–1025.
[89] Naguib M, Kurtoglu M, Presser V, Lu J, Niu J, Heon M, et al. Adv Mater 2011;23:4248–53.
[90] Lim KRG, Shekhirev M, Wyatt BC, Anasori B, Gogotsi Y, Seh ZW. Nature Synthesis 2022;1:601–14.
[91] Persson POÅ. In: 2D Metal Carbides and Nitrides (MXenes): Structure, Properties and Applications, eds. B. Anasori and Y. Gogotsi, Springer International Publishing, Cham, 2019, DOI: 10.1007/978-3-030-19026-2_8, pp. 125-136.
[92] Shahzad F, Alhabeb M, Hatter CB, Anasori B, Man Hong S, Koo CM, et al. Science 2016;353:1137–40.
[93] Tan TL, Jin HM, Sullivan MB, Anasori B, Gogotsi Y. ACS Nano 2017;11:4407–18.

[94] Ham DJ, Lee JS. Energies 2009;2:873–99.
[95] Liu Y, Kelly TG, Chen JG, Mustain WE. ACS Catal 2013;3:1184–94.
[96] Lee JS. Encyclopedia of catalysis 2002.
[97] Anasori B, Gogotsi Y. In: 2D Metal Carbides and Nitrides (MXenes): Structure, Properties and Applications, eds. B. Anasori and Y. Gogotsi, Springer International Publishing, Cham, 2019, DOI: 10.1007/978-3-030-19026-2_1, pp. 3-12.
[98] Shekhirev M, Shuck CE, Sarycheva A, Gogotsi Y. Prog Mater Sci 2021;120:100757.
[99] Barsoum MW, Eklund P. In: 2D Metal Carbides and Nitrides (MXenes): Structure, Properties and Applications, Anasori B, Gogotsi Y, editors, Springer International Publishing, Cham, 2019, DOI: 10.1007/978-3-030-19026-2_2, pp. 15-35.
[100] Anasori B, Xie Y, Beidaghi M, Lu J, Hosler BC, Hultman L, et al. ACS Nano 2015;9:9507–16.
[101] Naguib M, Mochalin VN, Barsoum MW, Gogotsi Y. Adv Mater 2014;26:982.
[102] Seidi F, Arabi Shamsabadi A, Dadashi Firouzjaei M, Elliott M, Saeb MR et al. Small, n/a, 2206716.
[103] Zhao S, Luo X, Cheng Y, Shi Z, Huang T, Yang S, et al. Chem Eng J 2023;454:140360.
[104] Wyatt BC, Rosenkranz A, Anasori B. Adv Mater 2021;33:2007973.
[105] Soni V, Singh P, Phan Quang HH, Parwaz Khan AA, Bajpai A, Van Le Q, et al. Chemosphere 2022;293:133541.
[106] Liu Z, Wu E, Wang J, Qian Y, Xiang H, Li X, et al. Acta Mater 2014;73:186–93.
[107] Verger L, Xu C, Natu V, Cheng H-M, Ren W, Barsoum MW. Curr Opin Solid State Mater Sci 2019;23:149–63.
[108] Dixit F, Zimmermann K, Dutta R, Prakash NJ, Barbeau B, Mohseni M, et al. J Hazard Mater 2022;423:127050.
[109] Rosen J, Dahlqvist M, Tao Q, Hultman L. In: 2D Metal Carbides and Nitrides (MXenes): Structure, Properties and Applications. Cham: Springer International Publishing; 2019. pp. 37-52.. https://doi.org/10.1007/978-3-030-19026-2_3.
[110] Ingason AS, Petruhins A, Dahlqvist M, Magnus F, Mockute A, Alling B, et al. Mater Res Lett 2014;2:89–93.
[111] Siebert JP, Mallett S, Juelsholt M, Pazniak H, Wiedwald U, Page K, et al. Mater Chem Front 2021;5:6082–91.
[112] Kuchida S, Muranaka T, Kawashima K, Inoue K, Yoshikawa M, Akimitsu J. Physica C 2013;494:77–9.
[113] Verger L, Natu V, Carey M, Barsoum MW. Trends Chem 2019;1:656–69.
[114] Zha X-H, Zhou J, Eklund P, Bai X, Du S, Huang Q. In: 2D Metal Carbides and Nitrides (MXenes): Structure, Properties and Applications, eds. B. Anasori and Y. Gogotsi, Springer International Publishing, Cham, 2019, DOI: 10.1007/978-3-030-19026-2_4, pp. 53-68.
[115] Hong W, Wyatt BC, Nemani SK, Anasori B. MRS Bull 2020;45:850–61.
[116] Sokol M, Natu V, Kota S, Barsoum MW. Trends in Chem 2019;1:210–23.
[117] Toth LE. J Less Common Metals 1967;13:129–31.
[118] Bortolozo AD, Sant'Anna OH, da Luz MS, dos Santos CAM, Pereira AS, Trentin KS, et al. Solid State Commun 2006;139:57–9.
[119] Lofland SE, Hettinger JD, Meehan T, Bryan A, Finkel P, Gupta S, et al. Phys Rev B 2006;74:174501.
[120] Sakamaki K, Wada H, Nozaki H, Ōnuki Y, Kawai M. Solid State Commun 1999;112:323–7.
[121] Bortolozo AD, Sant'Anna OH, dos Santos CAM, Machado AJS. Solid State Commun 2007;144:419-421.
[122] Bortolozo AD, Fisk Z, Sant'Anna OH, Santos CAMd, Machado AJS. Physica C: Superconductivity, 2009;469:256–258.
[123] Bortolozo AD, Serrano G, Serquis A, Rodrigues D, dos Santos CAM, Fisk Z, et al. Solid State Commun 2010;150:1364–6.
[124] Bortolozo AD, Sant'Anna OH, dos Santos CAM, Machado AJS. Mater Sci-Poland, 2012;30:92–97.
[125] Bortolozo AD, Osório WR, de Lima BS, Dos Santos CAM, Machado AJS. Mater Chem Phys 2017;194:219–23.
[126] Karaca E, Byrne PJP, Hasnip PJ, Tütüncü HM, Probert MIJ. Electronic Struct 2021;3:045001.
[127] Jin S, Su T, Hu Q, Zhou A. Mater Res Lett 2020;8:158–64.
[128] Fashandi H, Lai CC, Dahlqvist M, Lu J, Rosen J, Hultman L, et al. Chem Commun 2017;53:9554–7.
[129] Peng C, Wei P, Chen X, Zhang Y, Zhu F, Cao Y, et al. Ceram Int 2018;44:18886–93.
[130] Alhabeb M, Maleski K, Anasori B, Lelyukh P, Clark L, Sin S, et al. Chem Mater 2017;29:7633–44.
[131] Yu X, Cai X, Cui H, Lee S-W, Yu X-F, Liu B. Nanoscale 2017;9:17859–64.
[132] Ahmed B, Anjum DH, Hedhili MN, Gogotsi Y, Alshareef HN. Nanoscale 2016;8:7580–7.
[133] Natu V, Pai R, Sokol M, Carey M, Kalra V, Barsoum MW. Chem 2020;6:616–30.
[134] Liu N, Li Q, Wan H, Chang L, Wang H, Fang J, et al. Nat Commun 2022;13:5551.
[135] Zhao X, Holta DE, Tan Z, Oh J-H, Echols IJ, Anas M, et al. ACS Appl Nano Mater 2020;3:10578–85.
[136] Wang H, Wu Y, Xiao T, Yuan X, Zeng G, Tu W, et al. Appl Catal B 2018;233:213–25.
[137] Cao J, Li J, Li D, Yuan Z, Zhang Y, Shulga V, et al. Nano-Micro Letters 2021;13:113.
[138] Nemani SK, Zhang B, Wyatt BC, Hood ZD, Manna S, Khaledialidusti R, et al. ACS Nano 2021;15:12815–25.
[139] Yeh J-W, Chen S-K, Lin S-J, Gan J-Y, Chin T-S, Shun T-T, et al. Adv Eng Mater 2004;6:299–303.
[140] Ye YF, Wang Q, Lu J, Liu CT, Yang Y. Mater Today 2016;19:349–62.
[141] George EP, Raabe D, Ritchie RO. Nat Rev Mater 2019;4:515–34.
[142] Cai T, Wang L, Liu Y, Zhang S, Dong W, Chen H, et al. Appl Catal B 2018;239:545–54.
[143] Mei J, Ayoko GA, Hu C, Bell JM, Sun Z. Sustain Mater Technol 2020;25:e00156.
[144] Meshkian R, Tao Q, Dahlqvist M, Lu J, Hultman L, Rosen J. Acta Mater 2017;125:476–80.
[145] Tao Q, Dahlqvist M, Lu J, Kota S, Meshkian R, Halim J, et al. Nat Commun 2017;8:14949.
[146] Chen Z, Yang X, Qiao X, Zhang N, Zhang C, Ma Z, et al. J Phys Chem Lett 2020;11:885–90.
[147] Bai J, Zhao B, Lin S, Li K, Zhou J, Dai J, et al. Nanoscale 2020;12:1144–54.
[148] Naguib M, Halim J, Lu J, Cook KM, Hultman L, Gogotsi Y, et al. J Am Chem Soc 2013;135:15966–9.
[149] Zhao S, Meng X, Zhu K, Du F, Chen G, Wei Y, et al. Energy Storage Mater 2017;8:42–8.
[150] Naguib M, Mashtalir O, Carle J, Presser V, Lu J, Hultman L, et al. ACS Nano 2012;6:1322–31.
[151] Soundiraraju B, George BK. ACS Nano 2017;11:8892–900.
[152] Come J, Naguib M, Rozier P, Barsoum MW, Gogotsi Y, Taberna PL, et al. J Electrochem Soc 2012;159:A1368.
[153] Lind H, Halim J, Simak SI, Rosen J. Phys Rev Mater 2017;1:044002.
[154] Sarycheva A, Polemi A, Liu Y, Dandekar K, Anasori B, Gogotsi Y, et al. Advances 2018;4:eaau0920.
[155] Anayee M, Kurra N, Alhabeb M, Seredych M, Hedhili MN, Emwas A-H, et al. Chem Commun 2020;56:6090–3.
[156] Li Y, Shao H, Lin Z, Lu J, Liu L, Duployer B, et al. Nat Mater 2020;19:894–9.
[157] Kamysbayev V, Filatov AS, Hu H, Rui X, Lagunas F, Wang D, et al. Science 2020;369:979–83.
[158] Seredych M, Shuck CE, Pinto D, Alhabeb M, Precetti E, Deysher G, et al. Chem Mater 2019;31:3324–32.
[159] Huang S, Mochalin VN. Inorg Chem 2019;58:1958–66.
[160] Choi W, Choudhary N, Han GH, Park J, Akinwande D, Lee YH. Mater Today 2017;20:116–30.
[161] Wang F, Li J, Wang F, Shifa TA, Cheng Z, Wang Z, et al. Adv Funct Mater 2015;25:6077–83.
[162] Wu Y, Nie P, Wu L, Dou H, Zhang X. Chem Eng J 2018;334:932–8.
[163] Wang F, He P, Li Y, Shifa TA, Deng Y, Liu K, et al. Adv Funct Mater 2017;27:1605802.
[164] Ibrahim KB, Shifa TA, Moras P, Moretti E, Vomiero A. Small 2023;19:2204765.
[165] Chen C, Xie X, Anasori B, Sarycheva A, Makaryan T, Zhao M, et al. Angew Chem Int Ed 2018;57:1846–50.
[166] Wang X, Li H, Li H, Lin S, Ding W, Zhu X, et al. Adv Funct Mater 2020;30:0190302.
[167] Hu Z, Kuai X, Chen J, Sun P, Zhang Q, Wu H-H, et al. ChemSusChem 2020;13:1485–90.
[168] Mistry K, Jalja R, Lakhani B, Tripathi SS, Chandra P. Int J Hydrogen Energy 2022;47:41711–32.

[169] Pomerantseva E, Gogotsi Y. Nat Energy 2017;2:17089.
[170] Zhang Y, Yin L, Chu J, Shifa TA, Xia J, Wang F, et al. Adv Mater 2018;30:1803665.
[171] Wang F, Yin L, Wang ZX, Xu K, Wang FM, Shifa TA, et al. Adv Funct Mater 2016;26:5499–506.
[172] Shifa TA, Gradone A, Yusupov K, Ibrahim KB, Jugovac M, Sheverdyaeva PM, et al. Chem Eng J 2023;453:139781.
[173] Ibrahim KB, Shifa TA, Moras P, Moretti E, Vomiero A. Small 2023;19:2370002.
[174] Li B, Guo H, Wang Y, Zhang W, Zhang Q, Chen L, et al. NPJ Comput Mater 2019;5:16.
[175] Kim SJ, Koh H-J, Ren CE, Kwon O, Maleski K, Cho S-Y, et al. ACS Nano 2018;12:986–93.
[176] Lin H, Wang Y, Gao S, Chen Y, Shi J. Adv Mater 2018;30:1703284.
[177] Hemanth NR, Kim T, Kim B, Jadhav AH, Lee K, Chaudhari NK. Mater Chem Front 2021;5:3298–321.
[178] Tran PKL, Kim MS, Nguyen TH, Tran DT, Kim NH, Lee JH. Funct Compos Struct 2021;3:045005.
[179] Zhao M-Q, Xie X, Ren CE, Makaryan T, Anasori B, Wang G, et al. Adv Mater 2017;29:1702410.
[180] Xu E, Zhang Y, Wang H, Zhu Z, Quan J, Chang Y, et al. Chem Eng J 2020;385:123839.
[181] Li J, Rui B, Wei W, Nie P, Chang L, Le Z, et al. J Power Sources 2020;449:227481.
[182] Liu J, Liu Y, Xu D, Zhu Y, Peng W, Li Y, et al. Appl Catal B 2019;241:89–94.
[183] Li Y, Yang S, Liang Z, Xue Y, Cui H, Tian J. Mater Chem Front 2019;3:2673–80.
[184] Jiang W, Zou X, Du H, Gan L, Xu C, Kang F, et al. Chem Mater 2018;30:2687–93.
[185] Li Y, Ding L, Liang Z, Xue Y, Cui H, Tian J. Chem Eng J 2020;383:123178.
[186] Chen X, Wang S, Shi J, Du X, Cheng Q, Xue R, et al. Adv Mater Interfaces 2019;6:1901160.
[187] Van Der Zande AM, Kunstmann J, Chernikov A, Chenet DA, You Y, Zhang X, et al. Nano Lett 2014;14:3869–75.
[188] Howell SL, Jariwala D, Wu C-C, Chen K-S, Sangwan VK, Kang J, et al. Nano Lett 2015;15:2278–84.
[189] Jin J, Xiao T, Zhang Y-F, Zheng H, Wang H, Wang R, et al. Nanoscale 2021;13:19740–70.
[190] Sheikh ZA, Katkar PK, Kim H, Rehman S, Khan K, Chavan VD, et al. J Storage Mater 2023;71:107997.
[191] Samal R, Debbarma C, Rout CS. Catal Today 2023;424:113880.
[192] Li Y, Wu F, Qian J, Zhang M, Yuan Y, Bai Y, et al. Small Science 2021;1:2100012.
[193] Wally P, Ueki M. Wear 1998;215:98–103.
[194] H. Zhang, D. Zhu and C. Hu, in *Advances in Ceramic Matrix Composites (Second Edition)*, ed. I. M. Low, Woodhead Publishing, 2018, DOI: https://doi.org/10.1016/B978-0-08-102166-8.00014-1, pp. 331-354.
[195] Boller H, Hiebl K. J Alloy Compd 1992;183:438–43.
[196] Pang X, Wu T, Gu Y, Wang D, Che X, Sun D, et al. Chem Commun 2020;56:9036–9.
[197] Pang X, Lv Z, Xu S, Rong J, Cai M, Zhao C, et al. Energy Storage Mater 2023;61:102860.
[198] Beckmann O, Boller H, Nowotny H. Monatshefte für Chemie / Chemical Monthly 1970;101:945–55.
[199] Boller H. Int J Refract Metal Hard Mater 1993;12:195–7.
[200] Baaziz H, Ghellab T, Charifi Z, Güler M, Uğur Ş, Güler E, et al. Eur Phys J B 2023;96:55.
[201] Majed A, Kothakonda M, Wang F, Tseng EN, Prenger K, Zhang X, et al. Adv Mater 2022;34:2200574.
[202] Sakamaki K, Wada H, Nozaki H, Onuki Y, Kawai M. Molecular crystals and liquid crystals science and technology. section a. Mol Cryst Liq Cryst 2000;341:99–104.
[203] Iorio LE, Garrison JWM. ISIJ Int 2002;42:545–50.
[204] Suzuki M, Suzuki IS, Walter J. Phys Rev B 2005;71:224407.
[205] Jing Y, Liu J, Zhou Z, Zhang J, Li Y. J Phys Chem C 2019;123:26803–11.
[206] Zhang Y, Xu M, Zeng Q, Hao J, Li Y. Materials Today Electronics 2023;5:100053.
[207] Brec R, Ritsma J, Ouvrard G, Rouxel J. Inorg Chem 1977;16:660–5.
[208] Zhou W, Liu L, Zhu J, Tian S. Ceram Int 2017;43:9363–8.
[209] Hua M, Garcia CI, DeArdo AJ. Metall Mater Trans A 1997;28:1769–80.
[210] Dong F, Xue F, Du L, Liu X. J Alloy Compd 2015;620:240–8.
[211] Kurmaev EZ, Skorikov NA, Galakhov AV, Karimov PF, Galakhov VR, Trofimova VA, et al. Phys Rev B 2005;71:024528.
[212] Ibrahim KB, Shifa TA, Bordin M, Moretti E, Wu H-L, Vomiero A. Small Methods, n/a, 2300348.
[213] Zhang R, Tsai IL, Chapman J, Khestanova E, Waters J, Grigorieva IV. Nano Lett 2016;16:629–36.
[214] Weisskopf VF. Contemp Phys 1981;22:375–95.
[215] Shekhter RI, Yu G, Gorelik LY, Isacsson A, Jonson M. J Phys Condens Matter 2003;15:R441.
[216] A. J. Leggett, Berlin, Heidelberg, 1980.
[217] Walter J, Boonchuduang W, Hara S. J Alloy Compd 2000;305:259–63.
[218] Sakamaki K, Wada H, Nozaki H, Ōnuki Y, Kawai M. Solid State Commun 2001;118:113–8.
[219] Suzuki M, Suzuki IS, Noji T, Koike Y, Walter J. Phys Rev B 2007;75:184536.
[220] Ramalingam B, Vanek J, Maclaren JM, McHenry ME, Garrisonjr WM. Philos Mag B 2000;80:379–94.
[221] Mitro SK, Hadi MA, Parvin F, Majumder R, Naqib SH, Islama AKMA. J Mater Res Technol 2021;11:1969–81.
[222] Alonso-Lanza T, Aguilera-Granja F, González JW, Ayuela A. Physical Review Materials 2017;1:024001.
[223] González JW. J Phys Condens Matter 2019;31:125501.
[224] Yuan X, Chen Z, Huang B, He Y, Zhou N. J Phys Chem C 2021;125:10226–34.
[225] Zhao D, Zhou Y, Fan J, Liu T, Nie Y, Fu W, et al. Materials 2019;12:1118.
[226] Sakamaki K, Wada H, Nozaki H, Ōnuki Y, Kawai M. J Alloy Compd 2002;339:283–92.
[227] Wally P, Ueki M. J Solid State Chem 1998;138:250–9.
[228] Bai Y, He X, Zhu C, Chen G. J Am Ceram Soc 2012;95:358–64.
[229] Li J-F, Matsuki T, Watanabe R. J Mater Sci 2003;38:2661–6.
[230] Shuai C, He C, Peng S, Qi F, Wang G, Min A, et al. Adv Eng Mater 2021;23:2001098.
[231] Abdelkader AM. J Eur Ceram Soc 2016;36:33–42.
[232] Skarvelis P, Rokanopoulou A, Papadimitriou GD. Tribol Int 2013;66:44–8.
[233] Bandi WR, Krapf G. Analyst 1979;104:812–21.
[234] Duma AD, Wu Y-C, Su W-N, Pan C-J, Tsai M-C, Chen H-M, et al. ChemCatChem 2018;10:1155–65.
[235] Peng Q, Rehman J, Eid K, Alofi AS, Laref A, Albaqami MD, et al. Nanomaterials 2022;12:2825.
[236] Dinh KN, Liang Q, Du C-F, Zhao J, Tok AIY, Mao H, et al. Nano Today 2019;25:99–121.
[237] Ibrahim KB, Shifa TA, Bordin M, Moretti E, Wu H-L, Vomiero A. Small Methods 2023;7:2300348.
[238] Chala SA, Tsai M-C, Olbasa BW, Lakshmanan K, Huang W-H, Su W-N, et al. ACS Nano 2021;15:14996–5006.
[239] Zhao K, Ma X, Lin S, Xu Z, Li L. ChemistrySelect 2020;5:1890–5.
[240] Zhu J, Chroneos A, Schwingenschlögl U. physica status solidi (RRL) – Rapid Res Lett 2015;9:726–9.
[241] Zhao X, Zheng X, Lu Q, Li Y, Xiao F, Tang B, et al. EcoMat 2023;5:e12293.
[242] Zhao J, Wen J, Xiao J, Ma X, Gao J, Bai L, et al. J Energy Chem 2021;53:387–95.
[243] Yuan K, Hao P, Hu X, Zhang J, Zhou Y. J Mater Sci 2022;57:7001–11.
[244] Zhou J, Zha X, Zhou X, Chen F, Gao G, Wang S, et al. ACS Nano 2017;11:3841–50.
[245] Li N, Zhang Y, Jia M, Lv X, Li X, Li R, et al. Electrochim Acta 2019;326:134976.

[246] Ren CE, Zhao MQ, Makaryan T, Halim J, Boota M, Kota S, et al. ChemElectroChem 2016;3:689–93.
[247] Selvam NCS, Lee J, Choi GH, Oh MJ, Xu S, Lim B, et al. J Mater Chem A 2019;7:27383–93.
[248] Zhang C, Kim SJ, Ghidiu M, Zhao MQ, Barsoum MW, Nicolosi V, et al. Adv Funct Mater 2016;26:4143–51.
[249] Du C-F, Sun X, Yu H, Fang W, Jing Y, Wang Y, et al. InfoMat 2020;2:950–9.
[250] Lu M, Zhang Y, Chen J, Han W, Zhang W, Li H, et al. Journal of Energy Chemistry 2020;49:358–64.
[251] Zong H, Yu K, Zhu Z. Electrochim Acta 2020;353:136598.
[252] Patra A, Samal R, Rout CS. Catal Today 2023;424:113853.
[253] Huang Z, She S, Yang Y, Li Z, Long Y, Guo J, et al. Chin J Phys 2024;87:620–34.
[254] Sahoo R, Singh M, Rao TN. ChemElectroChem 2021;8:2358–96.
[255] Liu J, Liu X-W. Adv Mater 2012;24:4097–111.
[256] Wu M, Xin B, Yang W, Li B, Dong H, Cheng Y, et al. ACS Appl Energy Mater 2020;3:10695–701.
[257] Dymerska A, Kukułka W, Wenelska K, Mijowska E. ACS Omega 2020;5:28730–7.
[258] Maslana K, Wenelska K, Biegun M, Mijowska E. Appl Catal B 2020;266:118575.
[259] Pan J, Liu X, Ji H, Zhu Y, Zhuang Y, Chen K, et al. Chin Chem Lett 2024. https://doi.org/10.1016/j.cclet.2024.109515, 109515.
[260] Liu K, Cheng J, Yu Y, Sui Z, Guo F, Lei S, et al. Surf Interfaces 2024:103950.
[261] Li M, Li T, Jing Y. ACS Omega 2023;8:31051–9.